CHALMERS
UNIVERSITY OF TECHNOLOGY

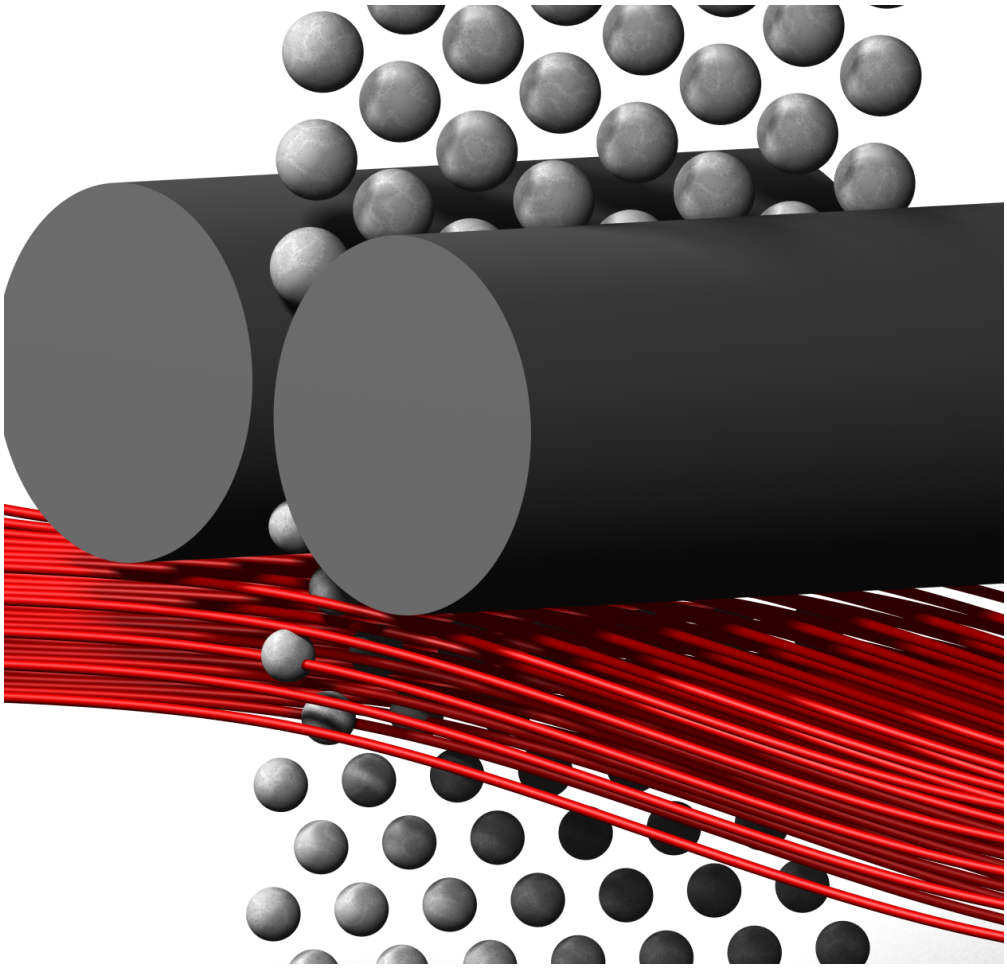

Thermo-Mechanical Integration of Waste Heat for Drying of Material during Milling

Master's thesis in Product Development

FILIP BOHM
HAMPUS TÄIKKÖ

DEPARTMENT OF INDUSTRIAL AND MATERIALS SCIENCES
CHALMERS UNIVERSITY OF TECHNOLOGY
Gothenburg, Sweden 2024
www.chalmers.se

Master's thesis 2024

Thermo-Mechanical Integration of Waste Heat for Drying of Material during Milling

FILIP BOHM
HAMPUS TÄIKKÖ

CHALMERS
UNIVERSITY OF TECHNOLOGY

Department of Industrial and Materials Science
Division of Product Development
Chalmers Rock Processing Research (CRPR)
Chalmers University of Technology
Gothenburg, Sweden 2024

Thermo-Mechanical Integration of Waste Heat for Drying of Material during Milling

FILIP BOHM & HAMPUS TÄIKKÖ

Supervisor: Clive Wynne, Comminution Reimagined Sweden AB
Examiner: Magnus Evertsson, Department of Industrial and Materials Science

Master's Thesis 2024
Department of Industrial and Materials science
Division of Product Development
Chalmers Rock Processing Research (CRPR)
Chalmers University of Technology
SE-412 96 Gothenburg
Telephone +46 31 772 1000

Cover: Airflow going through a curtain of material during crushing.

Typeset in LaTeX
Printed by Chalmers Reproservice
Gothenburg, Sweden 2024

Thermo-Mechanical Integration of Waste Heat for Drying of Material During Milling
Waste Heat Utilization for Enhanced Material Drying
FILIP BOHM
HAMPUS TÄIKKÖ
Department of Industrial and Materials Science
Chalmers University of Technology

Abstract

This thesis experimentally and theoretically investigated the integration of waste heat for drying of rock particles during milling, as well as the potential drying effect of heated airflows inside of Comminution Reimagined's ARBS mill. Pre-study tests indicate that a cost effective side effect, drying of the crushed particles, occurs when heat is added to the air system that extracts fine crushed rock particles. The drying of crushed particles is key in order to improve crushing performance and fines extraction. Previous research has left several knowledge gaps, mainly in terms of how the drying effect can be controlled and predicted, i.e. the drying parameters.

Experimental data was used together with a broad literature study to gain an understanding of the drying effect and parameters as. A conceptual design was created to illustrate a potential integration of the drying system for the current design of the rock crushing mill. Our findings indicate that integrating waste heat into the rock crushing mill can be done in an efficient way where the negative effects of moist rock particles inside of the ARBS mill can be minimised, but requires further research before implementation.

Keywords: Crushing, mill, drying, rock, waste, heat, sustainability.

Acknowledgements

We would like to express our sincere gratitude to our company supervisor Clive Wynne for helping the project move forward and always providing invaluable insights.

We would also like to thank our project supervisor Gauti Asbjörnsson for always being available with his guidance. Additionally, we would like to thank the engineering team at CR's Gothenburg office, Gustav Kolleby, Kristoffer Zietek, Jakub Ryż and Farshad Khorasani for their invaluable insights and continuous feedback during the project.

We would also like to thank Ezra Van Der Ven, a fellow master thesis student that we worked together with during the spring.

Lastly, we would like to extend our gratitude towards our examinator Magnus Evertsson for helping us realise this project. His aid extended well beyond what would be expected from his role as an examinator, for which we are grateful.

Filip Bohm & Hampus Täikkö, Gothenburg, June 2024

List of Acronyms

Below is the list of acronyms that have been used throughout this thesis listed in alphabetical order:

ARBS	Accurate Rock Breakage System
CR	Comminution Reimagined AB
FDM	Fused Deposition Modeling
PLC	Programmable Logic Controller
tph	Tonnes per hour

Terminology

Below is the list of terms that have been used throughout this thesis listed in alphabetical order:

Anemometer	A device that measures air velocity and direction.
Bridging	The blockading of the intake opening by particles. Whereas a single rock is small enough to pass through the crushing elements, they are prevented from doing so because of a buildup of material.
Fines	Small particles of crushed rock. They are typically the byproduct of rock crushing operations, although sometimes rock is specifically ground to produce these fine particles.
Flaking	Occurs When moist fines are compressed, and together form a hard flake.
FDM	Stands for Fused Deposition Modelling and is a common type of additive manufacturing principle where melted materials, most commonly different types of plastic, are laid on top of each other to form an object.
Formply	A plywood sheet with a phenol-formaldehyde resin coating.
Monolayer	A single, closely packed layer of entities. In this report, these entities are crushed rock particles.
Occupancy	How much of the space between the crushing elements that is occupied by material, and not air. Expressed as a percentage.
P-regulator	A p-regulator, or a proportional regulator, is a type of feedback control system used to maintain a desired output by adjusting a control variable.
U-type Manometer	A device consisting of a U-shaped tube filled with liquid, by measuring the height differences between the liquid pillars pressure difference can be calculated.

Contents

List of Figures

List of Tables

1
Introduction

This report aims to create an understanding of how this project was conducted and its findings, from thoughts and ideas to models, methods and results. First, in this chapter, the project scope and its limitations are presented, along with a description of the current products of the company.

1.1 Background

Crushing rock particles and other materials to fine sizes, typically below 150μm, is an essential preparatory step for the recovery of valuable minerals from the rock ores and is also used in many industrial processes. Comminution Reimagined Sweden AB (CR 2024a [3])(henceforth referred to as CR), has developed a low-energy, dry grinding technology for crushing material to fine sizes below 1mm, called ARBS (Accurate Rock Breakage System) (CR 2024b [4]). CR has proven the technology at a pilot plant in Northern Sweden and will potentially supply their first mill to a customer in Q3 2025.

CR's process has many benefits over existing crushing and milling technologies. However, the process is sensitive to the moisture content of the feed material, with a low moisture content being preferable, particularly in the final stages of crushing. In real-world conditions, mill feeds may exceed the optimal moisture content. Fortunately, the design of the CR mill may promote very effective drying if heated air can be introduced to the milling process, and CR's planned first customer has both a source of waste heat and a particularly demanding requirement for low moisture.

CR wishes to investigate the effectiveness of using such heated air to achieve the required level of drying and, if successful, incorporate air drying into its first mill. CR has already built a test chamber, the air rig, with precise measurement capabilities and has offered a Masters project in product development to demonstrate the feasibility of air drying, and, at a minimum, propose the necessary design modifications for the first mill.

The project was based at the company's laboratory in Gothenburg. The company envisaged immediately incorporating the design recommendations into its first mills, with respect to the results of the thesis.

1.2 Aim

The aim of this project are set out below.

- Measure the degree of drying that can be achieved under a range of operating conditions.
- Understand and quantify the operating parameters and machine design elements that enhance or diminish the drying effectiveness.
- Propose a set of changes to the mill design to enable the incorporation of effective air drying into the first mill.
- Ideally, incorporate the proposed changes into the final mill design (which would've had to be finalised by late May 2024).

1.3 Limitations

The limitations of the project are described in the list below.

- **Economic**. The project did not have a predetermined budget for either its development or the final deliverable. However, it was understood that any expenses incurred during the project had to receive approval and authorisation from CR. As the project progressed and a deliverable product took shape, i.e., a drying solution, it was essential to maintain active and dynamic collaboration with CR management and engineers to ensure that the project's costs remained within reasonable bounds and did not escalate excessively.
- **Time**. The final date for presenting the thesis was set by university guidelines for the 14th of June 2024, imposing a strict time constraint on the project's completion.
- **General Scope**. As this thesis project aimed at understanding and integrating the waste heat, it set a limit on what parts of the machine the outcome of this project could affect. For instance, if the thesis project deemed it necessary to change an integral part of today's ARBS, while it could be beneficial, limitations in both time and scope might have precluded extensive alterations and modifications to any subsystem of the current ARBS system.

2

Theory

In the following sections, the theory surrounding the project is laid out. The theory covers the ARBS mill, the air rig and a definition of sustainability, as well as a series of equations for mass balance, energy drop and pressure estimation. The theory was a result of the extensive literature studies conducted early on in the project.

2.1 Description of the ARBS milling principle

ARBS is a single particle monolayer rock crushing machine invented and developed by CR. The name ARBS stems from an acronymisation of *Accurate Rock Breakage System*. Single particle breakage in a monolayer has been shown to be the most energy efficient way to reduce particle size by compression. This crushing principle allows for greater precision in controlling the final particle size. The principle can be seen in figure 2.1

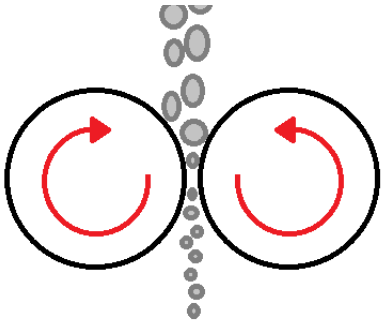

Figure 2.1: *Visualisation of the ARBS milling principle. The grey dots represent a falling curtain of rocks, getting crushed between a set of crushing elements. The gap size between these two sets the output particle size.*

2.1.1 Boliden pilot plant

The Boliden pilot plant is CR's scaled down ARBS-mill prototype, located in Boliden outside of Skellefteå. It consists of two mills, where the first one does pre-crushing and the second, larger mill, mills the feed down to the desired size. Material enters via a longer conveyor belt on to the first tower and then travels vertically in a curtain of particles between crushing elements with a decreasing gap. The material is then lifted vertically to and fed into the top of the larger mill where the material undergoes further crushing. The gap size between the crushing elements allows for

the material to get crushed until it comes out in particle sizes of 200-800 microns. There are inlets and outlets for air to suck particle fines out on the sides of the mill.

2.2 Drying parameters

This section covers the investigated drying parameters surrounding evaporation and vapour transportation.

2.2.1 Drying of materials

According to Tsotas et al. (2005)[5], the definition of drying is "the separation of volatile liquids from solid materials by vaporising the liquid and removing the vapour", and heat is required in order to vaporise a moist solid. A method without applied heat cannot strictly be defined as drying. It is mentioned that most moist materials have three drying phases where the drying rates differ. The first phase is when unbound liquid vaporises from the material's surface. For the second phase, as the surface of the solid dries out, liquid within cavities of the solid starts to vaporise. The third phase includes the vaporisation of the residual moisture, which have been sorbed by the material. During the first phase, the drying rate (which is the moisture loss over time) is said to be close to constant[5]. The drying rate decreases with the remaining moisture content during the second and third phase. It is also mentioned that during the first phase when surface evaporation takes place the properties of the material has no effect on the evaporation and only drying conditions effect the drying rate. In Solids drying: Basics and Applications (2014)[6], Parikh explains that the heat and mass transfer are critical factors while drying. Heat induces evaporation and the transfer of mass leads to the removal of vapour from the particle surface. Parikh (2014) also mentions that the inlet temperature and velocity also affect the moisture holding capacity of the gas. This will be further investigated in 2.5.3 with applied project dependencies.

2.2.2 Evaporation of moisture

According to the study carried out by Ajiwiguna and Putra (2017)[7] where the effects of the velocity and temperature of the airflow while drying farm products were analysed. Experimental data was gathered and showed that the temperature of the flow is less significant for evaporation when the airflow velocity is high. It also showed that evaporation tends to saturate at high temperatures for a constant air velocity.

2.2.3 Transportation of vapour

According to Libal (2018)[8], when drying a material by evaporating moisture, a transition from liquid to vapour takes place. This increases the humidity of the air. when the vapour is cooled down, the water condenses. When the amount of evaporation and condensation particles are the same, the air is saturated. This saturation is reached at the saturated vapour pressure P_s which depends on the temperature

T and can be found in table 1.1 in "Formel- och tabellsamling Termodynamik med Energiteknik"[9]. When the temperature increases, the saturated vapour pressure increases, which enables more vapour to occupy the air. The mass of vapour per volume air is called absolute humidity AH. The absolute humidity can be calculated from equation 2.1 [11].

$$AH = \frac{RH \cdot P_s}{R_w \cdot T \cdot 100} \tag{2.1}$$

RH is the relative humidity, which is defined as the percentile fraction of the mass of vapour currently in the air and the possible mass of vapour that can occupy the air. RH is equal to 100% as this yields the maximum vapour content of the air. R_w is the specific gas constant for water. This is 461,52 kJ/kgK [12]. A graph of the absolute humidity at different air temperatures can be seen in figure 2.2. It can be used to evaluate the volume of air needed at different temperatures to remove a certain mass of water vapour.

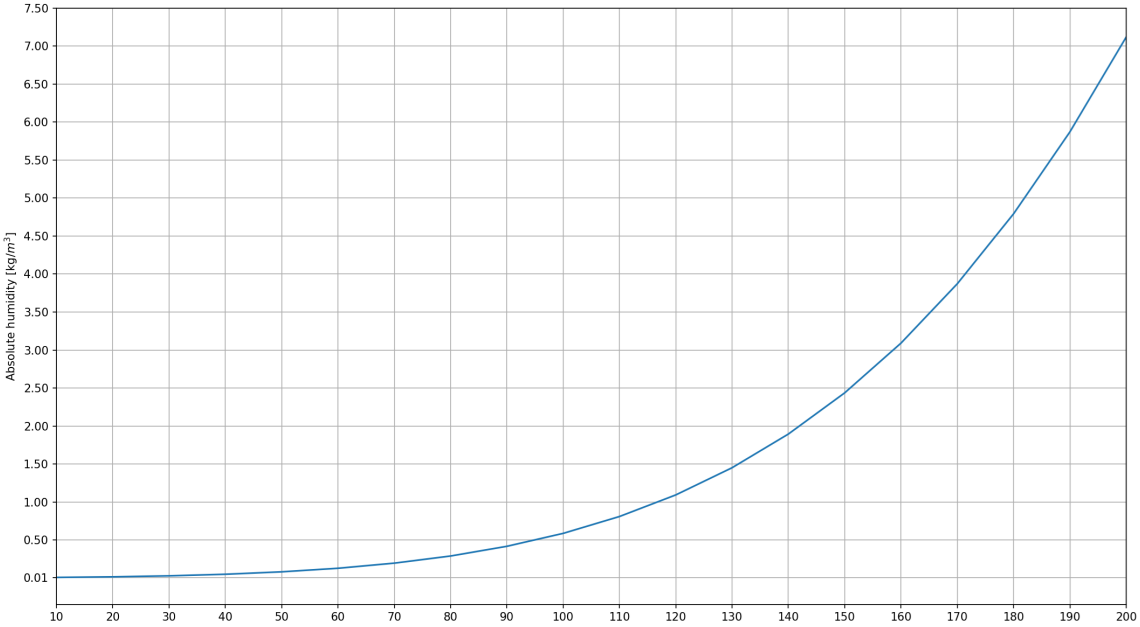

Figure 2.2: *Graph of the absolute humidity at different temperatures.*

A material feed rate $\dot{m}$ of 30 000 kg per hour was examined, as this is a realistic material feed rate for the pilot-sized ARBS mill, together with a material feed rate of 500 kg per hour, as this is the air rig feed rate given from the results of the material flow test (see 6.1). Moisture contents M_p of 3, 2 and 1% were set as these are realistic material moisture contents. This led to a mass of 900, 600 and 300 kg for the ARBS mill and 15,10 and 5 kg for the air rig of water that had to be removed per hour. By dividing the mass of water by the absolute humidity, the volumetric airflow needed to avoid vapour from condensation at different temperatures q_v could be calculated, see equation 2.2.

$$q_v = \frac{\dot{m} \cdot M_p}{AH \cdot 100} \tag{2.2}$$

The volumetric airflow to a void condensation at different temperatures for both the Boliden pilot plant and the local air rig are shown in graphs 2.3 and 2.4. The calculation does not take any losses into consideration or the effect of cool pipe walls, which could induce condensation. The calculations yields a rough estimation of theoretical flows and air temperatures needed to transport evaporated moisture from the air rig and the real life scenario. When running drying tests, the airflow and its temperature always exceeded the theoretical values to avoid condensation in the system. For future implementation at the Boliden pilot plant, this should also be taken into consideration when temperatures and airflow are set.

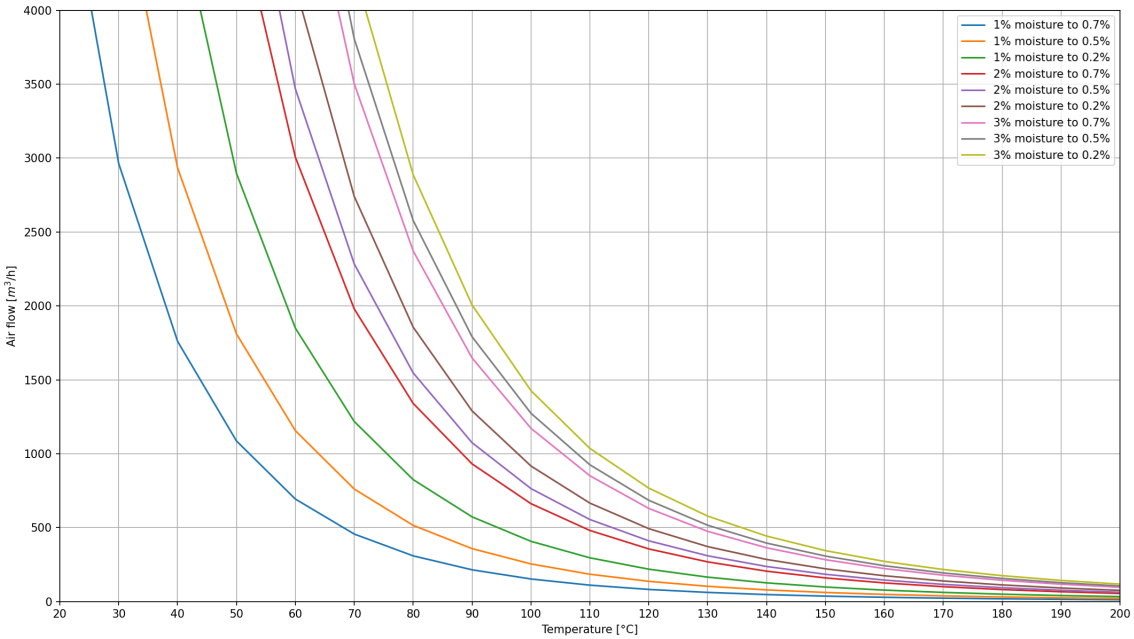

Figure 2.3: *Graph of the volume airflow at different temperatures needed to transport moisture from a material flow of 30000 kg per hour.*

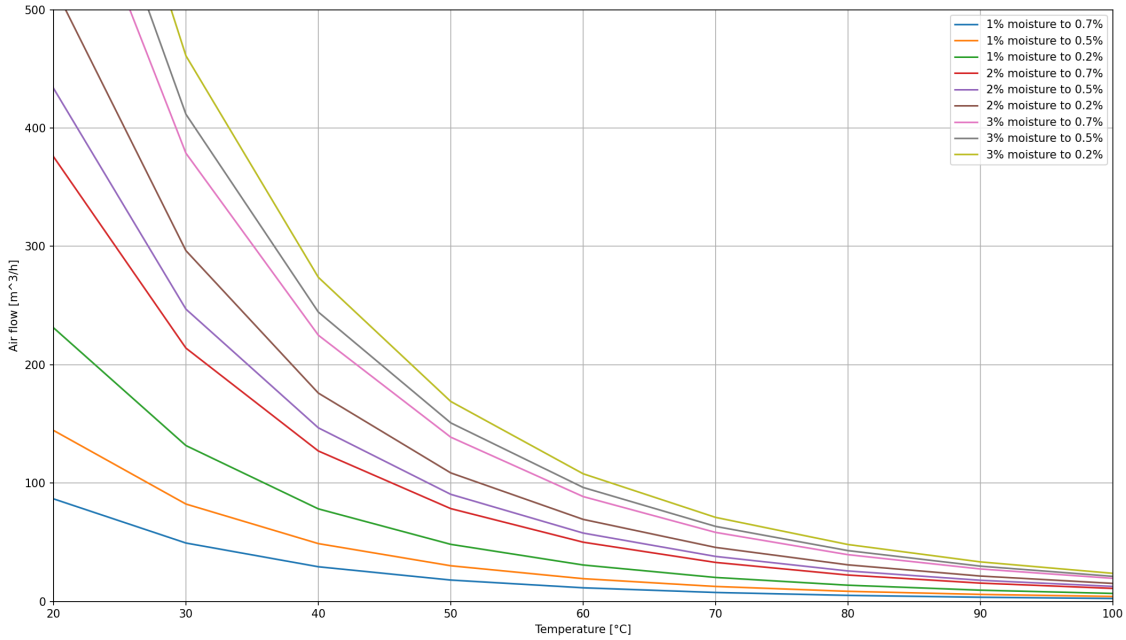

Figure 2.4: *Graph of the volume airflow at different temperatures needed to transport moisture from a material flow of 500 kg per hour.*

2.3 Dolomite

The mineral which the study has been carried out on is a limestone called dolomite. This mineral was used as it is one of the minerals which is currently being processed in the mills by a future potential company customer. The Mineral is also accessible for the work, as tests regarding wear of the crushing elements is being carried out with the mineral at the Boliden pilot plant. Dolomite is naturally colourless with a white or grey appearance, with some variation depending on impurities of other minerals. Other characteristics is its crystal structure and relative low hardness. according to Geo for CXC [13], limestone is a permeable mineral, meaning that liquid can be sorbed through cracks and pores. For this reason it must be taken into consideration that a significant amount of evaporation may occur in the second and third phase, as described in 2.2.1, where the drying rate is nonlinear.

2.4 Air rig

The drying of crushed rock particles is not the main reason to introduce air into the system. The removal of material fines has a significant impact on the forces introduced when breaking material, due to occupancy and flaking. In a previous project, a rig was built in order to observe how small material particles behave and can be removed in the machine utilising flowing air. This rig is referred to as the *Air rig*, see figure 2.5.

The air rig is a 1:1 scale accurate test rig of CR's working pilot plant in Boliden,

representing a reduced section of the pilot plant. The air rig consists of its crushing element surrounded by walls, on which airflow nozzles are mounted to allow for airflow through the machine. The nozzles direct the airflow through the curtain of material that falls downwards after the crushing process, which allows for the removal of fine particles. The walls are made of transparent plastic sheets in order to permit ocular observation of the particle behaviour.
The crushing elements are run by electric motors and the material is fed into the machine through a cap made from foam core on a conveyor. The material is evenly distributed onto the conveyor by a hopper, which holds material and has an adjustable gap. At the bottom off the machine, there is a collection bucket which has a foam core edge that it seals against the machine.

Crushing element speed and conveyor belt speed are controlled via a laptop using a web interface that connects to a PLC system. This PLC system can also read air velocities using a set of anemometers.

Vacuums ensure that the material fines can be collected from the material curtain, and a cyclone separates the material fines from the airflow, to ensure that the vacuum does not clog up.

Figure 2.5: *Picture of the air rig located in the lab at CR.*

2.5 Defining sustainability

The definition of sustainability is important due to the fact that it's a broad concept. It generally refers to the ability to "meet the needs of the present without

compromising the ability of future generations to meet their own needs". There is a need to translate this definition and apply it to the thesis project while at the same time taking into account how CR works with sustainability. Because of the nature of the technology that CR works with, sustainability is always present in their work. While the main sustainability focus is on the environmental and economical aspect, the potential effects of their ARBS mill will have consequences for general social sustainability as well. The sustainability aspect is evaluated further in section 6.10.

3
Methodologies

This chapter covers the different methodologies used in the project. A large part of the methods came from the need to perform tests, as the first and second aim (see 1.2) deals with understanding drying parameters and drying effect.

3.1 Project work plan

This project followed a work plan that was based on acquiring relevant knowledge in two ways: by conducting experiments and through literature studies. These two methods were both done continuously and parallel to each other, where findings from the experiments guided the progress in the literature studies and vice versa.

3.2 Material flow test

The lack of a belt scale by the slit on the hopper that feeds material to the conveyor belt made it exceedingly difficult to calculate and/or estimate the material flow, measured in tph (tonnes per hour). In order to determine the current material flow rate and set a future material flow rate, a series of 5 tests were conducted. The two variables for the material flow rate were the conveyor motor frequency, which is measured in hertz (Hz), and slit distance (mm) of the hopper that sits on top of the conveyor. The slit was set at 1,5 mm and the frequency was adjusted in between sending 3000 grams of material through the hopper. 3000 grams of material were used for each drying test, as a larger amount of material would compromise convenience of the test procedure, while a smaller test sample could yield skewed results. Together with a recording of the time it took for the material to pass the air rig, a tph could be determined. A material flow of 0,5 tph was then used for all drying tests evaluated in the 6.8.

3.3 Insulation test

Before implementing insulation in phase 3, a simple test were made in order to evaluate if the insulation could increase the input flow temperature by minimising the temperature drop through the inlet manifold and piping to it. The test was performed by connecting the industrial construction fan heater to a 1650 mm long duct pipe with a diameter of 100 mm which is the same size used for the manifold. At the other end of the pipe, the anemometer with built-in thermometer was placed

in the rig built to centre it to measure the outlet temperature. The inlet temperature were set to 60°C and regulated by the industrial construction fan heater, as this was the highest temperature the anemometer was specified for. The temperature of the environment was documented. The flow in the pipe created by the fan was measured at the end of the pipe. When the test started, it ran until the temperature readout at the pipe exit stabilised and was steady for five minutes. A complete test took one hour. And two tests were made, one with the 1650mm duct pipe with an insulation sleeve and one without.

Figure 3.1: *Insulation test setup, duct pipe without insulation to the left and duct pipe with insulation to the right.*

3.4 Rig temperature and heat permeability

The temperatures at the inlet of the rig was measured continuously for each drying test to ensure the desired temperature of the airflow, and to ensure comparability when alterations to the setup were implemented. The temperature measurements were also used to calculate and compare the energy balance between the phases. The temperatures at the inlet was measured with the thermal sensor in the industrial construction fan heater for each measurement in order to get consistent results. In combination with this, the outlet temperature was measured with the anemometer used for the velocity measurements, as it could do both velocity and temperature measurements simultaneously. The temperature of the environment were also documented in case it had an impact on the results. In phase 3, the test procedure was expanded to see how the temperature differed inside the rig. For this reason, four more test locations were added throughout the rig. These tests were carried out with a stick probe thermometer, which could be inserted into a small resealable hole to avoid leakage.

3.5 Air velocity probing tests

In order to gain a deeper understanding of the behaviour of the air flowing through the rig, a number of velocity tests were carried out during the duration of the

project. All velocities were measured using a hot wire anemometer of the brand Testo, model 405i. This anemometer allowed for live digital measurement readout. For consistent and repeatable measurements of the pipe flows a rig was constructed to hold the anemometer see figure 3.2. A plastic pipe for electrical installations were cut to perfect length to centre the anemometer and allow for its insertion. The pipe was then attached to a section of duct pipe to allow for mounting at desired measuring location. By assuming a fully developed pipe flow this is where the maximum velocity over the cross section is located. From the maximum velocity can the average velocity over the pipe cross section be calculated. This velocity can then be used to determine the mass flow of air. Extensions were placed in front of and after the anemometer to ensure a fully developed flow as bends can impact the velocity distribution over the pipe cross section.

Figure 3.2: *Centring rig for anemometer.*

Continuous measurements of the pipe flows at the in and outlet were performed to ensure stable conditions while performing drying tests. Velocity probing tests were carried out recurrently to observe and evaluate flow differences when performing changes to the rig. The first probing test were carried out at phase 2 to get a base measurement of the air rig. The second velocity probing test were carried out with different combinations of closing and keeping the bottom and top open of the rig in order to simulate an enclosed system and its effect on the airflow. With phase 3 a third probing was performed to compare the mass and energy balance to phase 2. The forth probing test were carried out on the manifold of the air rig to observe the distribution of airflow.

3.6 Pressure estimation and validation

Altering the pressure of a body of air will change its volume due to compression of its molecules. When this phenomenon occurs in a airflow the compression will result in a changed flow velocity. This phenomenon could explain the velocity difference between the inlet and outlet. The pressure needed for this volumetric change were calculated by assuming equal mass flow at the inlet and outlet. The validity of the estimation were then examined by measuring the real pressure difference between the inlet and outlet. For the measurement a U-type manometer were used [15]. This device utilise hydro static pressure to measure pressure differences. The manometer were constructed from a plastic hose. This hose were bent to a U-shape and filled with coloured water which creates two pillars. By exposing the ends of the hoses to different pressures the height of the pillars will change. By measuring the height difference between tests can pressure differences be calculated see figure 3.3 for visualisation of the U-type manometer.

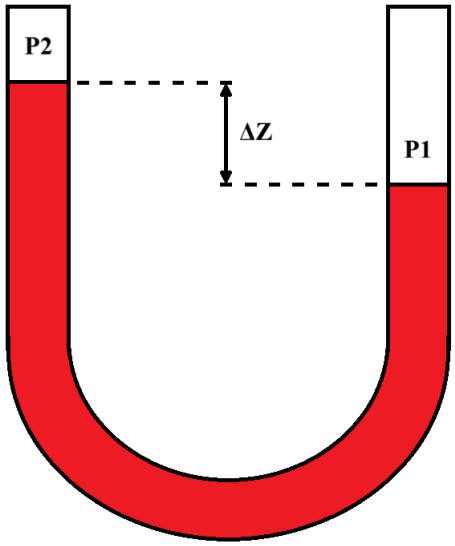

Figure 3.3: *Visualisation of a U-type manometer with a low pressure P_2, a high pressure P_1 and the height difference ΔZ of the pillars.*

The Pressure validation were performed at phase 2, and the test setup can be seen in figure 3.4. Initially, both sides of the hose were exposed to the atmospheric pressure at the inlet; for one pillar, the height of the surface were marked. One end of the U-type manometer were then exposed to the pressure of the outlet and height of the pillar surface was marked. A caliper were used to measure the difference between the marked lines.

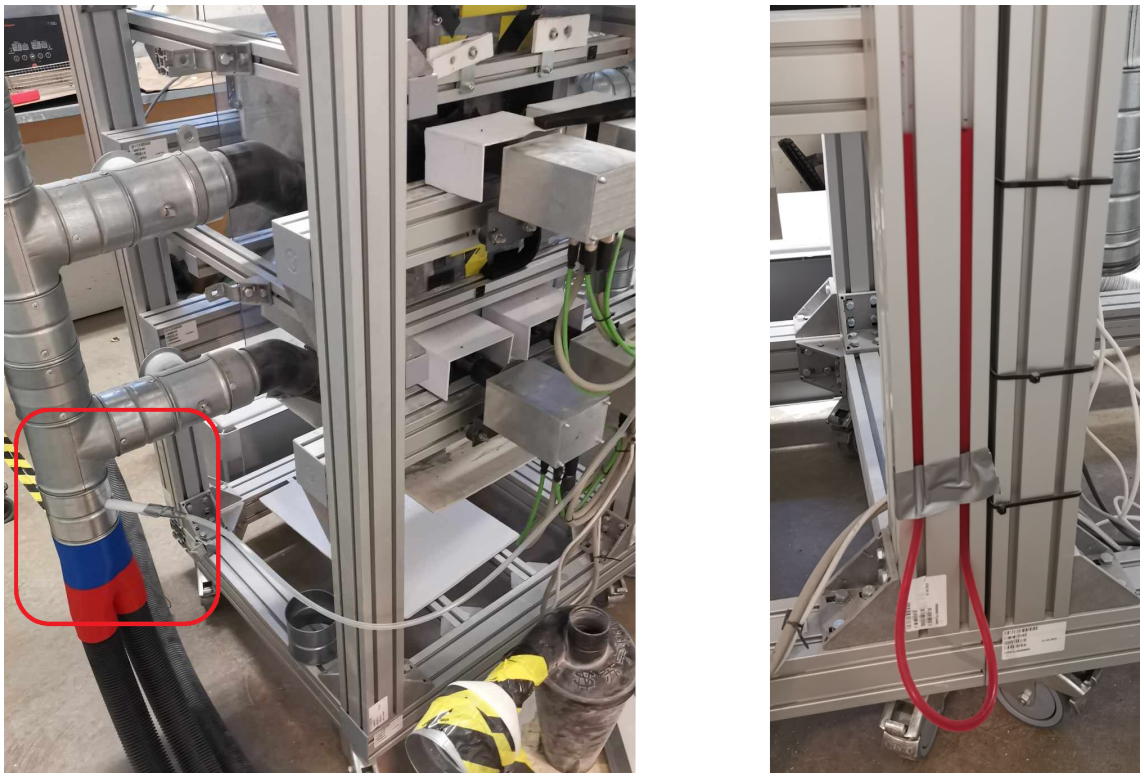

Figure 3.4: *U-type manometer setup with one hose end connected to the outlet, marked with red square, and one end exposed to atmospheric inlet pressure.*

3.7 Drying tests

Several drying tests were performed in order to observe how the drying parameters, temperature and flow velocity affect the moisture removal from the feed material. The test were carried out on the existing air rig, made to observe the behaviour of the airflow inside of the mill. The intention of performing tests on the existing rig was to see how much drying could be done in the current mill setup at the Boliden test plant. This laid the groundwork for the experimental data studied in the report. A test standard were created from the first drying test to ensure that all tests could be comparable to observe how test conditions altered the drying of material. An overview of the steps of a single test can be found in the list below, and a more detailed description of the different steps can be found below the list.

1. Weigh the total weight of the desired rock particles in a plastic bag
2. Add moisture until desired moisture content
3. Mix the bag properly and leave over night to ensure even distribution of the moisture in the particles
4. Setup the dry rig with correct conveyor speed
5. Set the desired temperature on the heater
6. Let the moist material run through the air rig
7. Record the time it takes for the moist material to pass through the machine
8. Weigh the moist material after it has gone through the air rig

9. Put the rock mix on a stainless steel tray and put it in a oven at 120°C for 12 hours
10. Weigh the material after it has been dried

The process of extracting valuable data from the air rig comes with several steps. Firstly, the type of material must be determined, which is based on what material the end customer of the ARBS mill processes. For the experiments conducted within the scope of this project, crystalline dolomite was the material type used in the tests. When the material is selected, its mass and desired moisture content needs to be decided. After measuring up the correct weight of the rock material, water is added to produce a mix.
Water needs to be added in order to simulate real-world scenarios where the material is seldom dry. The moist rock mix needs to be mixed properly to ensure an even distribution of moisture. This is done by rotating the bag manually and letting it sit overnight. The air rig has several input variables, such as conveyor belt speed, roller speed (the speed of the simulated crushing mechanism) and the distance between individual roller pairs. These are configured based on what type of test is running and gets noted down in a test sheet.

The rock material is placed in a hopper with a small duct at the bottom, which makes an even material flow on the conveyor belt possible. The second half of the setup are the vacuums and the heater. In order to dry the rock material, heated air is pulled through the air rig as it simulates getting crushed. There are several combinations of vacuums that allow for different airflows. The heater also allows for a wide variety of scenarios, as the temperature of its output can be set with a thermostat.

When the desired airflow and air temperature are correct, the conveyor belt is started and a stopwatch is used to record the time it takes for the rock mix to pass the air rig. When the rock mix has passed the air rig, it needs to be quickly put inside of an airtight container and weighted to ensure that no evaporation happens outside of the air rig. When all the rock mixes have gone through the air rig, they are evenly distributed onto individual stainless steel trays and put in an oven. The rock material is dried in the oven for approximately 12 hours at 120°C. When the rock material have dried, the weight is measured one last time in order to determine the initial moisture content, before adding in water.

3.8 Sieve analysis

A sieve analysis evaluates the particle size distribution of a granular material by passing it through a series of sieves with progressively smaller mesh sizes. This was performed in order to determine the particle size distribution of the dolomite in the laboratory at CR's Gothenburg office. The amount of material retained on each sieve is then weighed and expressed as a fraction or percentage, of the total mass. It is a common procedure in various fields, including civil engineering, geology, construction engineering and in the mining industry. An industrial mechanical shaker

of the brand Retsch with woven wire mesh sieves was used for the sieve analysis. Below is a step-by-step overview of how the sieve analysis was conducted at CR. The sieve analysis was performed in accordance to SS EN 033-1[17]

1. **Sample preparation**
   A fully representative sample of the granular material is collected using splitting, a method that ensures a representative size distribution of the sample. The sample needs to be of sufficient size to ensure accurate results but can not be to large, as it needs to fit the sieve analysis machine without overloading the sieve decks.

2. **Stacking sieves**
   The stack of sieves are placed on top of each other with the largest mesh size on the top and the smallest on the bottom and placed into the mechanical shaker.

3. **Weighing the sample**
   The total weight of the sample to be tested is measured and recorded onto a sieve analysis sheet.

4. **Shaking the sieves**
   The sample is place on the top sieve and the stack is subject to mechanical shaking and vibration for 30 minutes. This process allows particles to pass through the various sieves based on their sizes.

5. **Weighing the retained material**
   After the shaking, the material retained on each sieve is carefully collected and weighed. The weight of the material on each sieve is recorded.

6. **Data Analysis**
   The weight of the material retained on each sieve is used to calculate the percentage and fraction of the total sample that each sieve represents. These percentages are then plotted on a graph to create a particle size distribution curve

3.9 Interviews with engineers

Large amounts of the data and information surrounding the technology at CR were collected via meetings and daily interaction with the engineers at their Gothenburg office. These were often unplanned and unstructured, occurring when a need for clarification on a subsystem, performance data etc arose.

3.10 Data analysis method

This section covers the analysis of gathered data from all the different tests performed.

3.10.1 Air rig drying test data

All test data from the air rig drying tests was inserted into a spreadsheet software, Excel. When inserting the dry input mass of the material into the spreadsheet, equation 3.1 was used to calculate the moist input mass when a desired percentage of water were to be added to the dry input.

$$Moist\ input = \frac{Dry\ input}{1 - \frac{Moist\ percentage}{100}} \tag{3.1}$$

The percentile moisture content post drying of the material were calculated using equation 3.2.

$$Moisture\ post\ drying = \frac{Pre\ drying - Post\ drying}{Post\ drying} \cdot 100 \tag{3.2}$$

The reference value was calculated for each test series as the mass of water of the dry input with equation 3.3. The reference value were calculated from a sample without added moisture or drying through the air rig.

$$Reference\ value = Dry\ input - Post\ Drying \tag{3.3}$$

The initial percentile moisture content of the material were calculated using 3.4.

$$Initial\ moisture = \frac{Moist\ input - Dry\ input + Reference\ value}{Moist\ input} \tag{3.4}$$

A graph visualising the percentile moisture contents after drying at different temperatures and flow velocities were created in Python. Data points with multiple documented values were averaged before inserted into the graph.

3.10.2 Airflow test data

All test data from the airflow tests were evaluated in the spreadsheet software Excel.

3.10.3 Sieve analysis

A paper template provided by CR were used to document the weight measurements for each mesh size. These values were then inserted into a Excel spreadsheet. The weights were summed up and subtracted from the initial sample weight. The difference were denoted as loss and assumed to be particles smaller than the smallest mesh size. The percentile distribution was calculated for each mesh size. The fraction of loss were added to the smallest particle fraction. From the percentile distribution, the cumulative distribution calculated for each mesh size by summarising the fractions of mesh sizes smaller or equal to itself. Graphs of the particle size mass

distribution, cumulative particle size distribution and percentile material loss were created using Python.

3.11 Sustainability - Use2use

Use2use is a method for evaluating concepts with regard to sustainability. It does this by reviewing the concept in three aspects, "*Is it preferable for the user(s)?*", "*Is it a smart move for the organisation?*" and "*Is it good for the environment?*". These are in turns split into the application's potential as well as the implementation.

4

Product Concept

This chapter covers the customers needs via a requirement specification, concept generation and evaluation. The chapter concludes with the selection and description of a final concept.

4.1 Customer needs

The different stakeholders voiced many similar needs. While CR required a lot of drying in order to keep the efficiency of the machine high, the customer only needed a fraction of that drying in order to not clog up the transport between the ARBS mill and the subsequent step in the production chain. These differing reasons, demands and wishes were collected and written down over the course of several weeks.

4.2 Requirement specification

The aforementioned demands and wishes were subsequently compiled in a requirement specification (4.1) shown below. The full requirement specification with descriptions, target values and verification method can be found in the appendix A. The requirement specification took both the customers and CR's demands and wishes into account and laid the foundation for the concept evaluation.

Table 4.1: Requirement specification.

Number	Name	Stakeholder	Demand/wish	Weight factor
	Moisture Content			
1	Material moisture content out	CR	D	
2	Material moisture content out	Customer	D	
3	Material moisture content in, demand	CR	D	
4	Material moisture content in, wish	CR	W	3
	Temperatures			
5	ARBS mill core temperature	CR	D	
6	Conveyor belt heat	CR, Customer	W	3
7	Input airflow temperature	CR, Customer	D	
	Cost			
8	Proposed concept cost, demand	CR, Customer	W	2
9	Proposed concept cost, wish	CR, Customer	W	2
	Time			
10	Effective drying time	CR, Customer	D	
	Particles			
11	Allowed particle size for air removal	CR	D	
	Environmental			
12	Energy consumption, waste heat	Customer	W	3
13	Energy consumption, additional energy	CR, Customer	W	3
14	Energy efficiency	Customer	W	3
15	Under-pressure in mill	CR	D	
	Construction			
16	Ease of assembly	CR, Customer	W	3
17	Compatible with current system	CR, Customer	D	
18	Resistant to dust	CR, Customer	D	
19	Resistant to outdoor environments	CR, Customer	D	
	Maintenance			
20	Maintenance interval concurrency	Customer	W	2
21	Ease of part replacement	CR, Customer	W	2
	Safety			
22	Low risk of injury	Customer	D	5
	Operation			
23	Easy to operate	Customer	W	3
24	Adjustable drying	Customer	W	3
24	Predictive drying	CR, Customer	W	4

4.3 Concept generation

This section covers the concept generation phase of the project. With established requirements for the product, the process of generating ideas for a drying concept

4.3.1 Black box

A black-box diagram (fig 4.1) was created to simplify, define and visualise system inputs and outputs without specifying the internal structure. This was done in order to show the flow and transformation of the green inputs to the red outputs that the system should enable without delving into intricate details. The black-box diagram shows how the drying system for rock milling inputs material, hot air and energy and transforms it into a refined milled product, material fines, water extracted from the material, dry air and waste heat from the process.

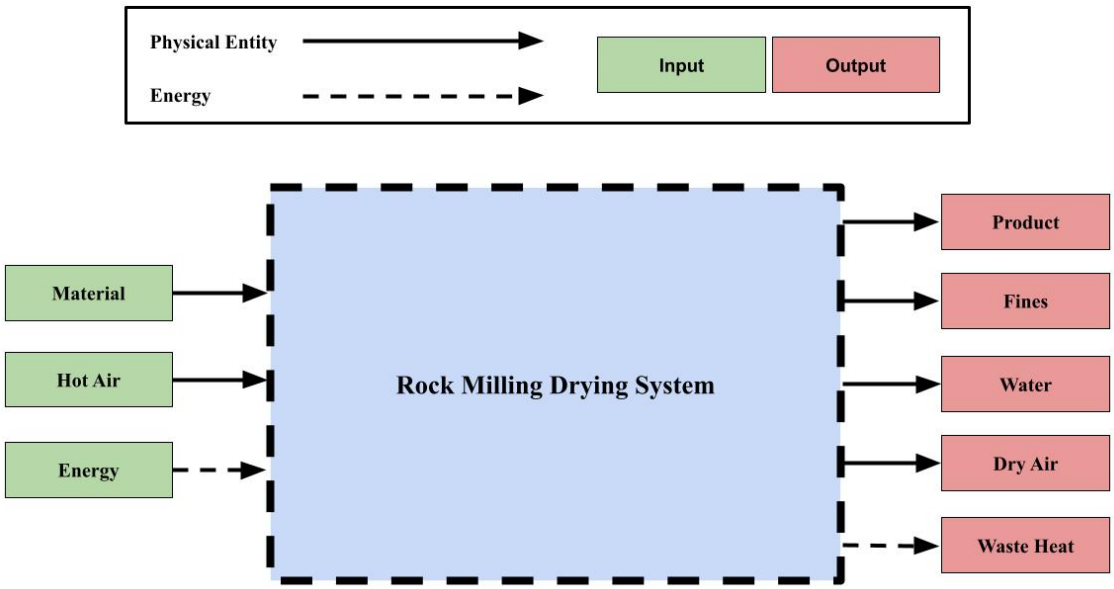

Figure 4.1: *Black-Box Diagram*

4.3.2 Functional structure

From the black-box diagram, a simple functional structure (fig 4.2) was created in order to understand the rough functions of the system and how these interact by visualising the flow of physical entities, energy and how these change the inputs of the system into the outputs through functions. The intention was that this understanding of the system would lead to higher quality concepts during the brainstorming session. The system and module boundary are visualised with blue and green dotted lines. The drying system is marked with a red dotted line.

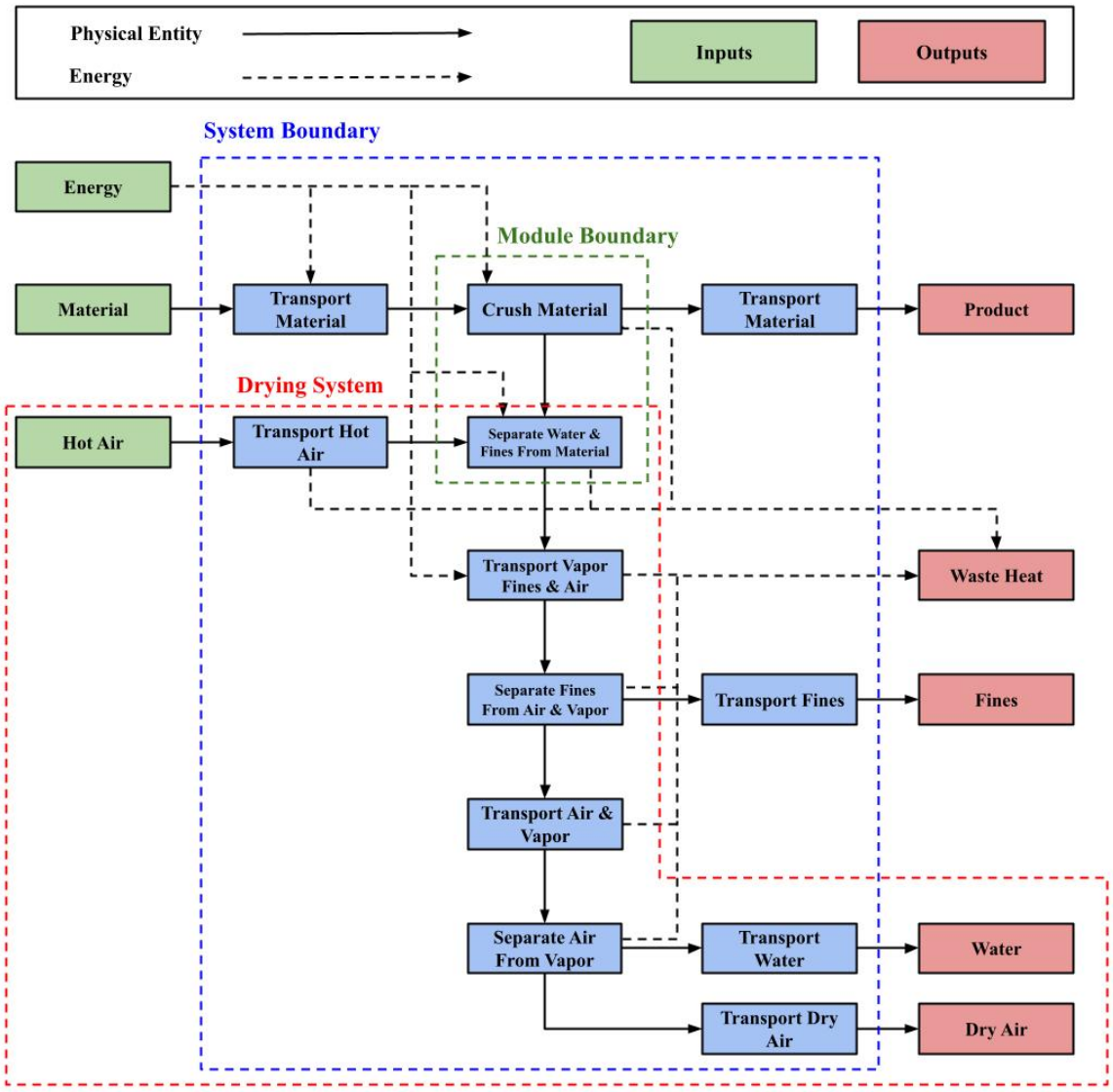

Figure 4.2: *Functional structure.*

Unprocessed material is transported into the machine and enters the module, where it is crushed to it's final particle size. Moisture and material fines are then separated from the material using hot air. The finished product is then transported from the module. The hot air in the system is transported to the module, where it separates the moisture and fines from the material. The hot air turns the moisture into vapour. The vapour and fines are transported with the hot air. Then, fines are separated and transported out of the system. The air and vapour are transported. The water and air is separated and both transported out of the system.

4.3.3 Brainstorming

Concepts and possible solutions to promote the drying of material passing through the system were generated through several brainstorming sessions. During these brainstorming sessions, all thoughts and ideas were taken into account, and pessimistic thinking was avoided, as even ideas with flaws could have yielded insight or

had the potential to evolve into something useful. This kind of thinking supports creativity. The brainstorming session led to the creation of 19 concepts. A brief description of each concept can be found below:

Concept 1 is called tumbler. The material is fed through an incline drum. A hot airflow is applied in the opposite direction to create a cross flow. The drum is rotated to expose more surface area of the material.

Concept 2 is called symmetry flow vacuum. Air is sucked out in a symmetrical manner from below the rolls.

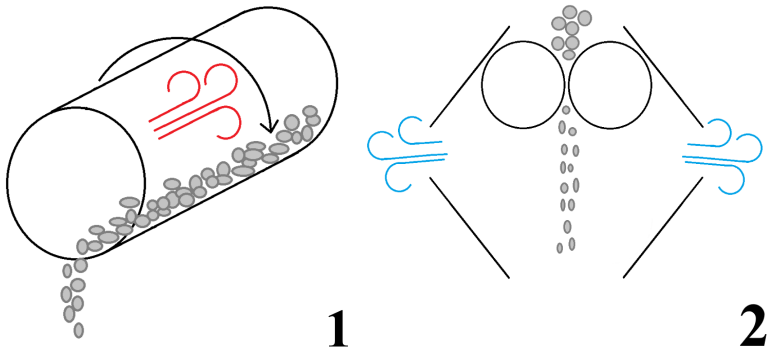

Figure 4.3: *Concept 1, 2.*

Concept 3 is called symmetry flow blow. Hot air is blown in a symmetrical manner on both sides onto the material curtain exiting the rolls to vaporise moisture.

Concept 4 is called rotation air in rolls. Hot air is blown onto the material curtain below the rolls. The humid air is then sucked out of the system. To take advantage of the heat that the airflow has when exiting the air is circulated back into the system.

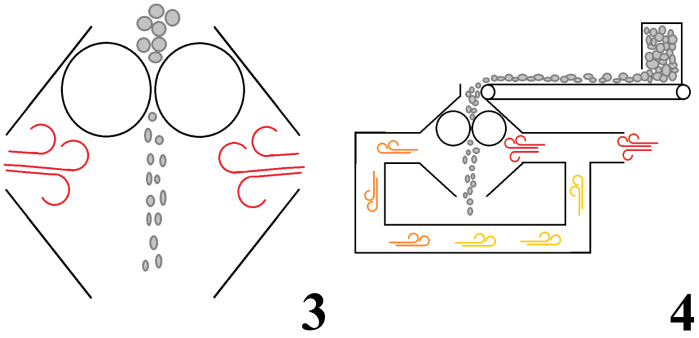

Figure 4.4: *Concept 3, 4.*

Concept 5 is called Ribs on conveyor. By adding ribs to the transporting conveyor

more surface area of the pebbles entering the system is exposed which could increase drying when applying a heated airflow.

Concept 6 is called heated rolls. The rolls are heated as the material is milled by the rolls the thermal conduction is high and moisture in the material is vaporised. The vapour is then sucked out by a vacuum from below the rolls.

Concept 7 is called heat from above. Hot air is blown onto the material before entering the rolls to evaporate moisture before milling takes place. The humid air is then sucked out with a vacuum from below the rolls.

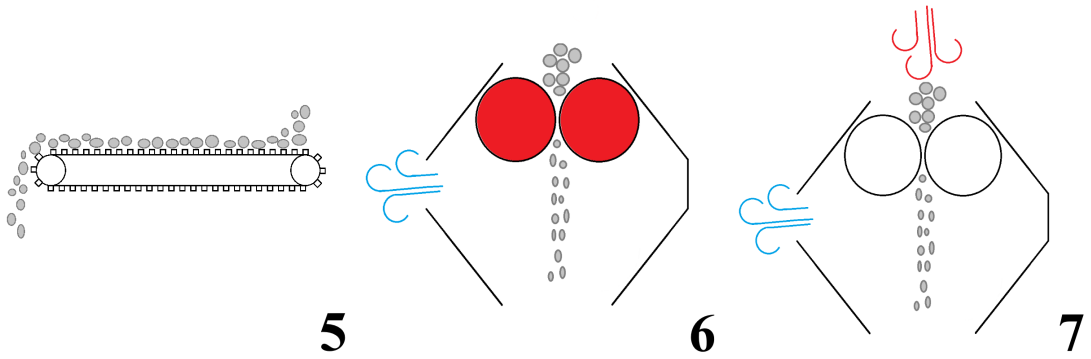

Figure 4.5: *Concept 5, 6, 7.*

Concept 8 is called enclosed system by material in hopper. Hot air is blow onto the entering material, to accumulate the heat the transport conveyor between the hopper and the system is enclosed. The hopper is also sealed by utilising the feed material.

Concept 9 is called perforated vacuum conveyor. Material is transported within an encasement on a conveyor. The conveyor has perforations which lets air pass through. A stream of hot air is blown in the opposite direction to the material flow to create a counter current to increase the thermal exchange. A vacuum is applied within the conveyor so that the airflow will exit through the perforations and remove moisture.

Concept 10 is called enclosed perforated conveyor. Material is transported within an encasement on a conveyor. The conveyor has perforations which let air pass through. A stream of hot air is blown through the conveyor to that the material is heated from below. Moisture is vaporised and is removed by a exerting airflow.

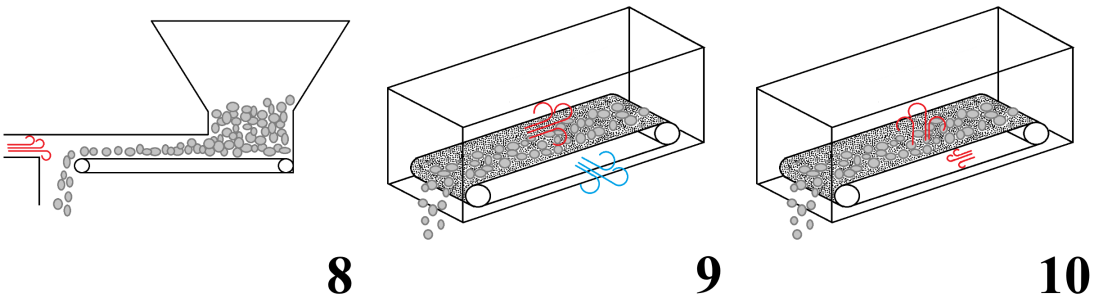

Figure 4.6: *Concept 8, 9, 10.*

Concept 11 is called enclosed conveyor. Material is transported within an encasement on a conveyor. Hot air is blown in the opposite direction of the material flow to create a cross-current to increase thermal exchange. Moisture from the material is vaporised and exits the encasement with the airflow.

Concept 12 is called enclosed conveyor freeze. Material is transported within an encasement on a conveyor. The temperature within the encasement is low enough so that the moisture in the material will freeze avoiding the negative effects of milling wet material.

Concept 13 is called drying by increasing occupancy. By moving the rollers closer together during the milling process the amount of space between particles decreases, with this the force increases. Kinetic energy is transformed to thermal energy and water inside the material will vaporise either due to the increased thermal energy or the pressure increase.

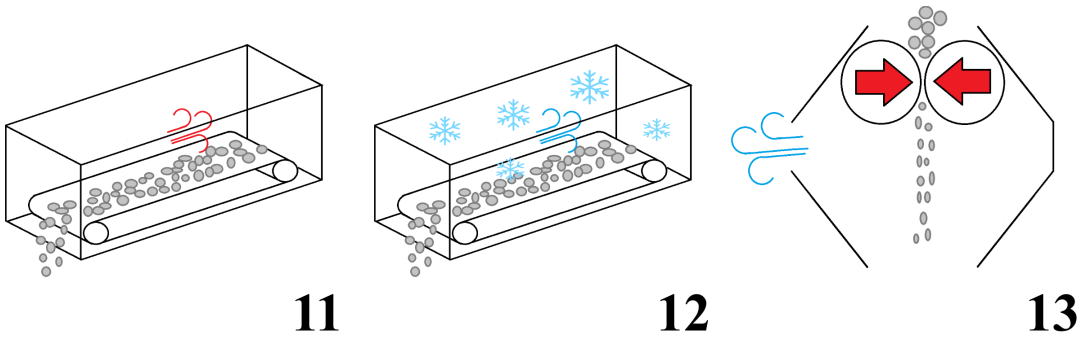

Figure 4.7: *Concept 11, 12, 13.*

Concept 14 is called cross-flow in machine. Hot air is blown onto the material curtain below the rollers. The humid air then exits the system by using a vacuum.

Concept 15 is called multiple levels of conveyors. Conveyors are stacked within an encasement to increase the time for drying before entering the system. Inside the

encasement, there is a stream of hot air to vaporise the moisture from the material. The air then exits to remove the vapour.

Concept 16 is called air on conveyors then rollers. Waste heat is blown onto the entering material and is transported and blown onto the material curtain. The humid air is then removed by suction.

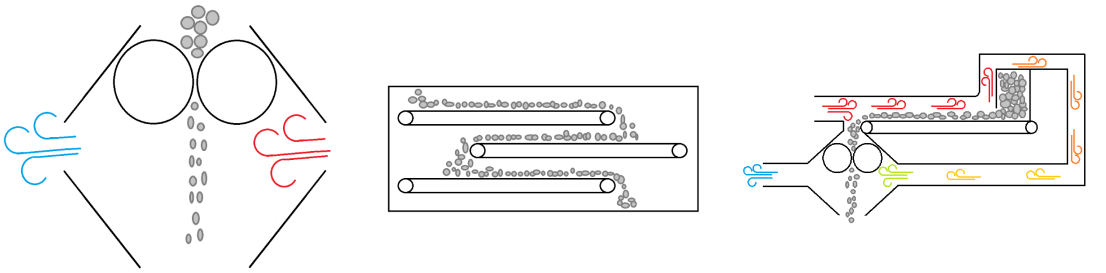

Figure 4.8: *Concept 14, 15, 16.*

Concept 17 is called separate air on rollers and conveyor. Waste heat is separately blown onto the material curtain below the rollers and the material before it enters the system. The air is sucked out to remove the humid air.

Concept 18 is called air on rollers then conveyors. Waste heat is blown onto the material curtain below the rollers the air then exits and is transported onto the pebbles entering the machine so they are partly dried before entering the system. Cold air and vapour then exit the system. The air is more hydrated at the end of the system but as the material flow acts in the opposite the drying will still take place.

Concept 19 is called addition of drying media. This concept utilises a solid drying media. The particles of the drying media is dispensed from a hopper and mixed with the pebbles from the material flow. Moisture is then transferred from the pebbles to the drying media. The mixture of drying media and pebbles are then transported by conveyors to a perforated track. The particles of the drying media are small enough to fall between the perforations, which separates the drying media and the pebbles. The moisture that the drying media has sorbed is vaporised by a hot airflow and then the particles are circulated back into the system.

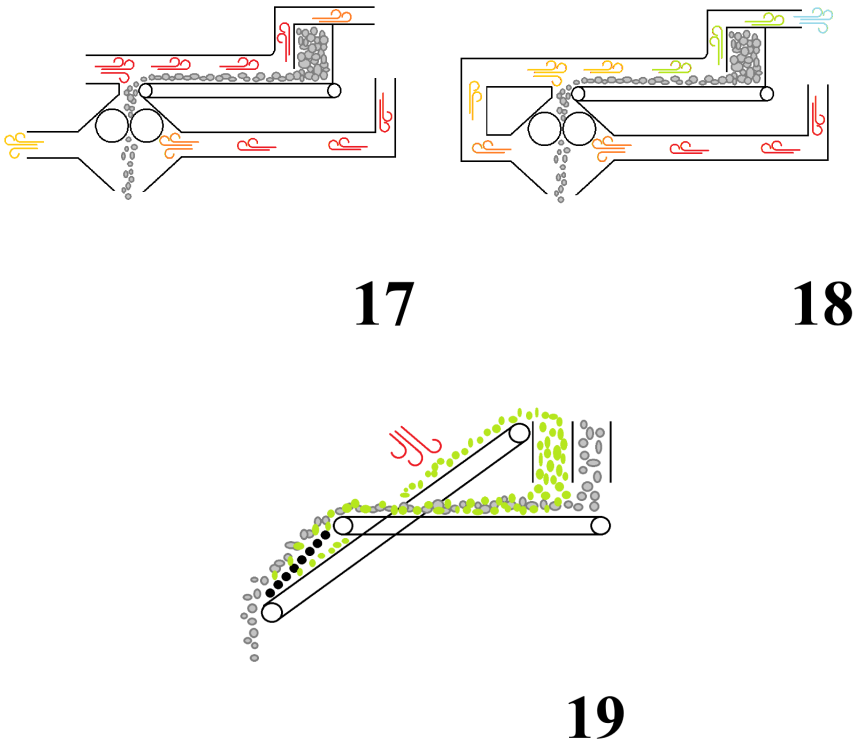

Figure 4.9: *Concept 17, 18, 19*

4.4 Concept evaluation and elimination

This section covers the concept evaluation and elimination. The concepts were reduced from 19 to a final concept. First, an elimination matrix was used to effectively reduce the number of concepts. Following the elimination matrix, a Pugh revision was performed to further reduce the number of concepts left. At the end of the Pugh matrix, a single concept remained.

4.4.1 Elimination matrix

An elimination matrix is a broad method used to reduce the number of concepts in a product development framework. It works by setting up a number of criteria based on the requirement specification (see tab. 4.1) where a concept is eliminated if it does not fulfil a set criteria. This method of initial screening was general, as several requirements required further research before they could be properly used to evaluate concepts.

Table 4.2: Elimination matrix with the generated concepts.

CHALMERS	*Elimination Matrix*															*Latest revision date: 2024-03-16*	
Concept	**Feasible**	**Compatible with Current System (Replaces current part)**	**Low Operator Injury Risk**	**Simple**	**Waste Heat Incorporated**	**Energy Efficient**	**Reliable and Durable**	**Complies with Safety Standards**	**Complies with Regulation**	**Easy to Integrate**	**Technologically Mature**	**Cost-effective**	**Scalable Solution**	**Low Environmental Impact**	**Long Maintanance Interval**	Elimination Criteria: [+] Yes [-] No [?] More information required [!] Check product specification Decision [+] Proceed with concept [-] Eliminate concept [?] Seek more information [!] Check product specification	
																Comment	Decision
1	+	-	+	+	+	-	+	+	+	+	+	-	+	-	+		-
2	+	+	+	+	-	+	+	+	+	+	-	+	-	+	+	Drying possible without added heat?	?
3	+	+	-	+	+	+	+	+	+	+	-	+	-	-	+		-
4	-	+	-	-	+	+	+	+	+	-	+	+	-	-	+	overpressure in machine	-
5	?	-	+	+	+	+	+	+	+	+	?	+	+	+	+	Does it yield a positive drying effect?	?
6	-	-	+	-	+	+	-	?	+	-	-	?	-	+	-		-
7	-	+	+	+	+	+	+	+	+	-	-	+	-	+	+		-
8	+	+	+	+	+	+	+	+	+	+	+	+	+	+	+		+
9	+	-	+	+	+	+	+	+	+	+	+	+	+	+	+		+
10	+	-	+	+	+	+	+	+	+	+	+	+	+	+	+		+
11	+	+	+	+	+	+	+	+	+	+	+	+	+	+	+		+
12	-	-	+	-	-	-	-	+	+	-	+	-	+	-	?		-
13	-	+	+	-	-	-	-	+	+	-	-	+	-	-	-		-
14	+	+	+	+	+	+	+	+	+	+	-	+	-	+	+		+
15	+	+	+	-	+	?	+	+	+	-	+	?	+	?	+	Several conveyors neccesary?	?
16	+	+	+	+	+	+	+	+	+	+	-	+	+	+	+		+
17	+	+	+	+	+	+	+	+	+	+	-	+	+	+	+		+
18	+	+	+	+	+	+	+	+	+	+	-	+	+	+	+		+
19	?	-	+	-	+	+	?	+	+	-	-	-	+	-	-		-

After the elimination matrix, it became clear that many of the brainstormed concepts seemed feasible. Using the 15 different criteria in the elimination matrix only reduced the brainstormed concepts from 19 to 9. Concepts *2*, *5* and *15* needed further research before a decision could be made.

As concept *2* (see fig. 4.3) did not utilise the waste heat, it was important to quickly determine whether or not drying could be possible with cold air. As this took place early on in the project, a general lack of knowledge regarding drying parameters and drying effects led to a shorter evaluation of current market solutions, where most seemed to rely on heat to be able to vaporise and transport the moisture away. Because of this, the concept was eliminated.

Concept *5* (see fig. 4.5) relied on heating the crushing elements, which in turn would dry the crushed particles while simultaneously letting an air stream flow over the material curtain. Because of the cautiousness required around the many sensors in the machine in terms of heat, it was deemed not worth it to pursue an idea that required the fine balance of heating the crushing elements up to a point where they could successfully dry the crushed material and not overheat any of the sensors. More research into the possibility of drying using the crushing element was not conducted due to the aforementioned reasons.

The research conducted for concept *15* (see fig. 4.8) showed that similar industrial solutions exist, but the cost of implementing a drying solution where the current conveyor belt would have to be replaced with a multi-layer conveyor dryer was deemed prohibitive.

4.4.2 Pugh matrix

With the concepts reduced to 9 remaining ones, a Pugh matrix iteration was performed to further reduce the number of concepts. Concept *11* (see fig. 4.7) was chosen as the reference concept due to its exceptional results in the elimination matrix. New criteria were selected based on the performed elimination matrix and the requirement specification (4.1). Concepts *14* and *17* were the only 2 concepts to outperform the reference.

Table 4.3: Pugh matrix iteration of the concepts.

CHALMERS	*Pugh Matrix 1*								
Latest revision date: 2024-03-18									
Requirements	**Concepts**								
	11	8	9	10	14	15	16	17	18
Feasability		-	-	-	0	-	-	+	-
Compatability with current system		-	-	-	+	-	0	0	0
Simplicity	R	-	-	-	-	-	-	-	-
Energy efficiency	E	+	+	+	+	-	+	+	+
Integrability	F	0	-	-	+	-	0	0	0
Technological maturity	E	0	0	0	0	0	0	0	0
Low cost of implementation	R	-	-	-	+	-	0	0	0
Environmental impact of implementation	E	0	0	0	+	-	0	+	0
Maintanance and effect on current maintanance schedule	N	0	0	0	0	-	0	0	0
Have enough information	C E	-	+	0	0	0	0	0	0
Σ +		1	2	1	5	0	1	3	1
Σ 0		4	3	4	4	2	7	6	7
Σ -		5	5	5	1	8	2	1	2
Net value		−4	−3	−4	4	−8	−1	2	−1
Rank		**6**	**5**	**6**	**1**	**8**	**3**	**2**	**3**
Comment		Vapour removal?							
Decision		Rem.	Rem.	Rem.		Rem.			Rem.
Reflection	Combining different solutions to cover more of the design space?								

At this point in the project, the vapour removal calculations 2.2.3 were completed and it was evident that the removal of vapour would be more important than previously expected. Because of this realisation, concept *8* was removed regardless of where it would be ranked in the Pugh matrix.

4.4.3 Final concept elimination

Similarities within the three well performing concepts (*11*, *14* and*17*) gave birth to the idea that these could be combined. While concept *17* already is essentially a combination of concepts *11* and *14*, it was not evident from the Pugh matrix alone whether or not a single concept would be better than a combined one. Due to the expected inexpensiveness of adding conveyor drying and the positive effects of drying

material before it is crushed, it was decided that all of these 3 concepts would be chosen as the final concept. The strength of the chosen concept grows when looking at the potential heat provided, while the mill itself can only withstand temperatures upwards of 80°C, the conveyor belt and its component can withstand temperatures above 120°C. This results in the possibility to receive a high temperature airflow and split it up where the warmest air stream gets sent to the conveyor, and a cooler air stream gets sent to the mill.

4.5 Final concept

The final concept was called *separate air on rollers and conveyor*, concept number 17 (4.9), where waste heat is separately blown onto the material curtain below the crushing elements and on the material on top of the conveyor belt before it enters the mill. The drying inside of the machine uses piping already present on the ARBS mill for fines extraction, with an added layer of insulation around the pipes.

The conveyor belting is performed with a counter current airflow going across the feed material, where simple conveyor covers with outer insulation is fitted on top of the longer conveyor belts. These covers ensure that the heated air does not leak out to the atmosphere.

5
Air rig prototyping

This chapter covers the prototyping, rebuilding and upgrading of the air rig. Some upgrades were minor improvements, while others completely remodelled the integral parts of the air rig. This chapter initially lays out the initial conditions for the air rig.

5.1 Initial conditions

The air rig was built for studying airflow inside the mill and was therefore not fitted to experiment using heat. The initial air rig lacked a heat source, proper sealing around the mill and heat insulation in the piping transporting the air.

5.2 Phase 1

The first phase of prototyping and upgrading was initiated by adding a heat source in the form of a 2200 W heat gun mounted at the inlet of the initial air rig in order to observe if there was any increase in drying going from a non heated airflow to a heated airflow through the material curtain.

When discussing the initial airflow results with the engineers at CR and if the low inlet velocity could be due to leakages and if the air tightness was inadequate. A lack of air tightness would result in air getting pulled from the outside of the air rig, which leads to a lower airflow through the inlet where the heater is situated and in turn, a lower flow through the material curtain with a lower temperature. This could directly lead to lower drying performance.

In order to improve the air tightness of the air rig, an initial upgrade was designed and implemented. The initial upgrades consisted of improving the bearing shaft sealing around the crushing elements using adhesive sheets of vinyl as well as sealing openings where air could enter with vinyl tape.

5.3 Phase 2

The second phase started off by replacing the mounted heat gun with a modified construction fan heater see figure 5.1. This heater consisted of two 9 kW construction

fan heaters which were connected in series in order to increase the ability to heat the flowing air. This fan heater was also equipped with a P-regulator, which controlled the heating elements using a temperature sensor positioned in the heated airflow. The regulator could then be set to different temperatures, which gave the ability to accurately test different temperatures at different airflow velocities. The accuracy of the temperature sensor was confirmed using an infrared thermometer. The modified heater showed early problems as the internal thermostats had been left inside of it, which shut it off when it reached temperatures higher than one heater supported. For this reason, the thermostats were disconnected. Another problem was an automatic safety thermostat, which, at high temperatures, would shut off due to it running for a long period of time. To avoid this problem without inducing a fire hazard, the heater was disconnected in between tests.

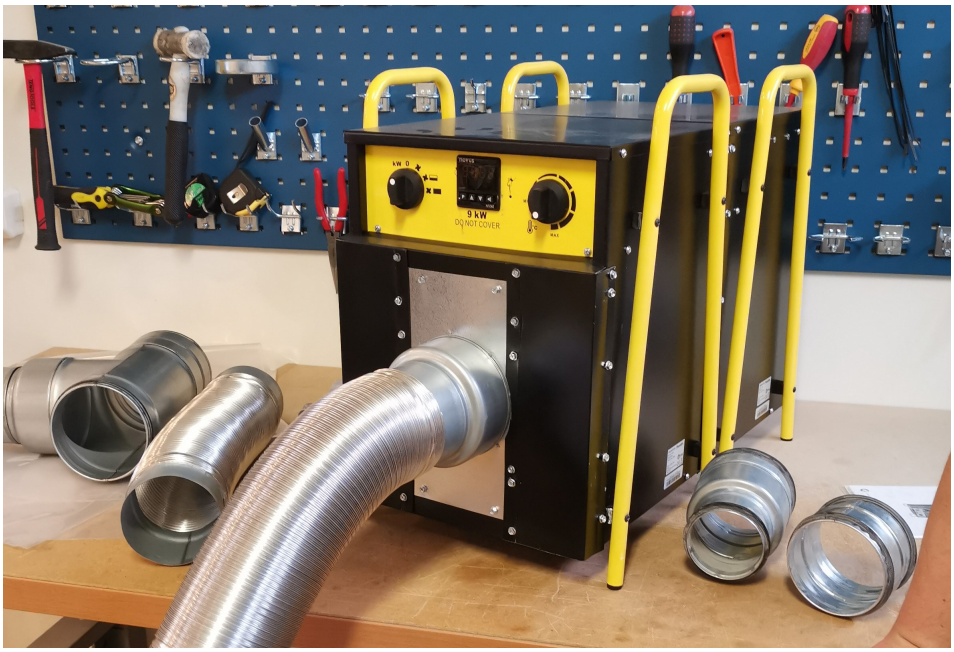

Figure 5.1: *Modified construction fan heater.*

In order to observe how increased airflow at the outlet would effect the drying and flow through the rig, a second vacuum was connected to the outlet. To get effective airflow and air tight coupling between the rig and the vacuums A Y-cross connection was designed using CAD software and manufactured through FDM. The Y-cross was constructed to support an interior tight press fit from a 100 mm ventilation pipe connector in one end, allowing for connection to the air rig, and in the other end with two custom thread connections that matched the threaded hoses on the vacuums, allowing for their assembly. Dimensions for the connections and threads were iterated using test parts until satisfactory fitment was archived. Internal edges were avoided and smooth transitions were made to reduce flow friction losses. The Y-cross was also designed for robustness, avoiding supports, and reducing material and manufacturing time.

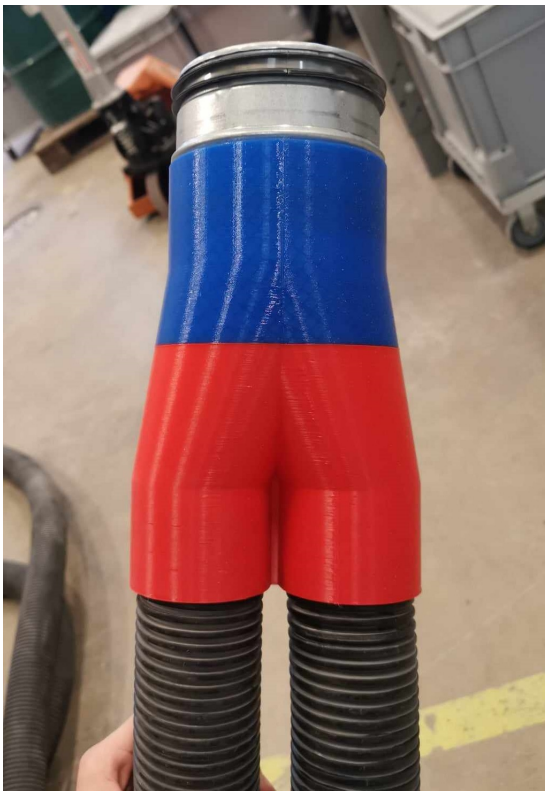

Figure 5.2: *Y-cross connection for the connection of two vacuums onto the outlet of the rig.*

5.4 Phase 3

The third phase started with a redesign of the crusher shaft seals in order to improve the sealing performance of the ones made from vinyl sheeting, as the friction from the spinning shafts, together with dust and heat, compromised the adhesion of the vinyl sheets. An iterative development of the shaft seals started with a two-part design with a rigid housing made with PLA and a flexible sliding seal out of TPU, which is well suited for gaskets (see fig. 5.3). Both parts were designed for FDM. The sliding seal was constructed with a 20-mm hole in the centre, allowing the shaft to pass through. The inside of the hole was designed with lips in order to yield a tight seal to the shaft while avoiding inducing friction

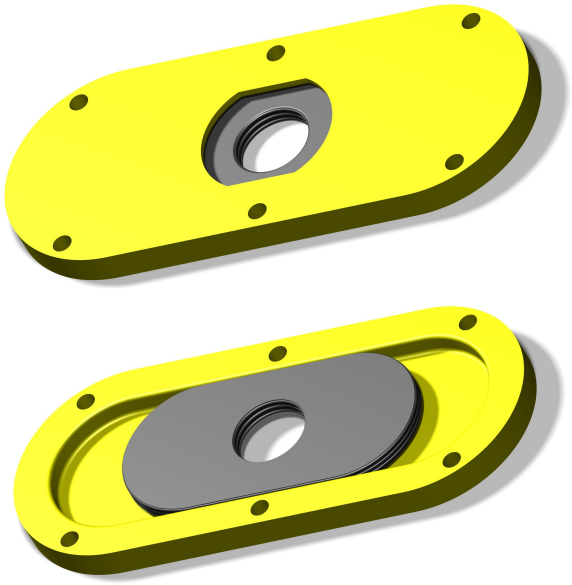

Figure 5.3: *The first design iteration of the shaft seal is a two-part design including a rigid housing and a flexible sliding gasket.*

The outside and top of the sliding seal were also designed with lips to seal against the housing. The housing was slotted, allowing for the seal to move horizontally, allowing for adjustment of the roller gap. Six mounting holes were also added to the housing for fasteners. After the seal housing was manufactured, it was realised that the design was too complex, making it impractical for efficient implementation due to time constraints and potential functional risks.

To reduce the complexity a new design were made including only one component, see figure 5.4. At this moment a decision had been made to move the walls of the air rig closer to the rollers to get a more efficient airflow through the material curtain. The rollers were mounted on the roller shafts with locking screws. These locking screws passed through the walls of the rig with the shorter wall-to-roller distance. To avoid collision between the seal and the locking screws a wider section was made to the seal. The design was manufactured with PLA through FDM. The seal had a brim with slotted holes allowing for mounting and horizontally movement to alter the roller gap. The sealing principle of this design built upon having a hole with minimal clearance which the shaft could pass through.

Figure 5.4: *The second design iteration of the shaft seal, a one part design utilising a minimal clearance fit for sealing against the shaft.*

After evaluation of the design of the second seal a decision was made to do a last iteration with the same sealing concept as it was not possible to mount the second seal due to its size and it being not sturdy enough. This resulted in the third and final seal iteration, see figure 5.5. This design had slotted countersunk holes allowing for the use of m5 hex screws for fastening and it moving horizontally. in the centre of the seal a hole with minimal clearance was placed for the shaft to pass through. Chamfers were added to the hole to ease the shaft assembly. The final seal design was originally made out of PLA, when testing the seal it was apparent that friction was a problem. An attempt to run in the seals by spinning the shafts with an electrical drill and adding oil reduced some friction, but it had to be reduced further to not risking burning a motor. Another seal was created using the material PET-G and the friction caused from rubbing was reduced significantly. After running it in with oil it gave a satisfactory seal and a low shaft friction.

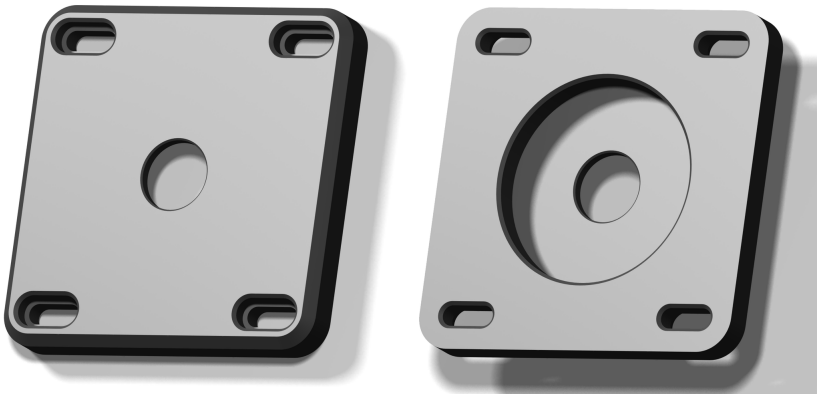

Figure 5.5: *The third design iteration of the shaft seal, a size optimised one part design utilising a minimal clearance fit for sealing against the shaft.*

As mentioned, upgrades were made to the walls, in order to reduce leakages and induce airflow through the material curtain. A Parallel project had yielded indications that air was travelling in the gap between the wall and the rollers instead of

through the material curtain, which could lead to inefficient drying. By reducing the wall-to-roller gap, this was assumed to be avoided. This was achieved by replacing the initial walls consisting of three plastic sheets to a solid sheet of formply. By cutting out the chamber geometry the walls were able to be moved closer together, while reusing parts needed to mount the initial sides and nozzles with only minor modifications to save on time for redesign and manufacturing. The solid walls gave more stability which enabled the walls to be mounted on the same aluminium profile as the bearing seats for the roller shafts. Holes were drilled for observing temperature differences in the air rig while drying with a needle thermometer. The holes were plugged with M4 screws.

As the velocity test showed the highest flow velocity at the inlet when closing the hopper and bottom, a encasement of the conveyor was made that both sealed to the hopper and to the top of the rig. The only opening was the hopper slit which was covered by material when the hopper is filled, closing the system. The encasement was equipped with an acrylic window at the top to view the feed material. The bottom was also improved, this was done by making a track for the collection bucket to slide into, the top of the track was covered in sealing foam, which pushed against the collection bucket creating a tight seal. A smaller bucket was also used which would fit 20L material instead of the previous 88L. This would allow for a more convenient test procedure due to the sample size of 3000g of dolomite.

The manifold and pipe between the inlet and the modified construction fan heater was insulated using rock wool duct insulation sleeves as the insulation test indicated that a significant amount of heat could be retained from insulation.

When all the modifications in Phase 3 had been completed, an acrylic sealant was applied to all gaps to prevent any air from entering the chamber.

6

Results & analysis

This chapter covers the results and analysis from material flow, insulation and temperature, Air velocity probing and the air rig drying tests. It also presents the sustainability evaluation with the Use2use method.

6.1 Material flow test

The material flow test (fig. 6.1) resulted in an understanding of how the parameters of material flow could be altered. The results also played an important role in visualising and relating the scale of the air rig to the actual material flow in the ARBS mill and the Boliden test plant, where the ARBS mill has a material flow circa 60 times the air rig and the Boliden test plant circa 4 times greater.

Table 6.1: Material flow test results.

Material input[g]	**Time [s]**	**Motor frequency [Hz]**	**Feed rate [tph]**
1001,20	69	3	0,05
1000,30	28	9	0,13
1000,70	14	18	0,26
1000,00	7	36	0,51
3000,20	22	36	0,51

6.2 Insulation test

The Insulation test orienting map in figure 6.1 visualises the measuring locations for the insulation test results presented in 6.2. These showed an increase in temperature with 5 °C over a duct pipe distance of 1650 mm when adding standard air ducting insulation to the 100 mm diameter duct pipe while running a low velocity flow through, which could be measured to about 1 m/s, together with an inlet flow temperature of 60 °C. An increase of the surrounding temperature with 2,3 °C was also apparent due to weather conditions which could have affected the results.

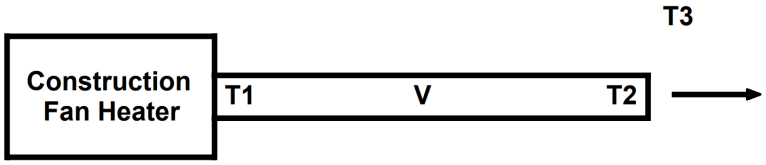

Figure 6.1: Insulation test orienting map.

Table 6.2: Insulation test results.

Test	T1 [°C]	T2 [°C]	T3 [°C]	V [m/s]
No Insulation	60	42	23,4	1,1
Insulation	60	47	25,7	1,2

6.3 Rig temperature and heat permeability

The temperature test orientation map In figure 6.2 shows the location of the measured temperatures in table 6.3 from phase 2 and table 6.4 from phase 3. From these temperature measurements, a decrease in temperature difference between T1 and T2 could be seen from phase 2 to 3, suggesting lower thermal losses. The extensive temperature measurements throughout the air rig in phase 3 suggest that the inlet manifold distribute more heat into the lower part of the rig, As the temperatures T3, T4, T5, and T6 consistently showed increasing temperatures from T3 as the lowest to T6 as the highest.

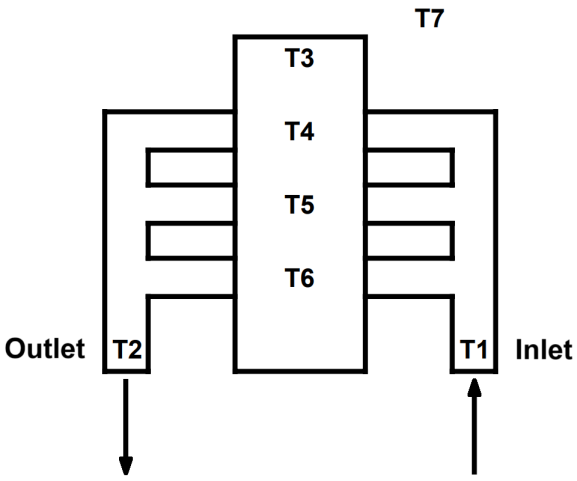

Figure 6.2: Temperature test orienting map.

Table 6.3: Temperature test results phase 2.

Test	T1 [°C]	T2 [°C]	T7 [°C]
4	40	28,0	22,0
4	50	32,0	21,9
4	60	34,0	22,0
4	70	38,5	22,0

Table 6.4: Temperature test results phase 3.

Test	T1 [°C]	T2 [°C]	T3 [°C]	T4 [°C]	T5 [°C]	T6 [°C]	T7 [°C]
6	25,0	25,0	25,7	25,6	25,2	25,2	25,4
6	40,0	33,5	27,8	28,5	34,3	36,0	26,7
6	60,0	43,9	28,7	30,6	48,0	51,0	27,3
6	80,0	51,6	29,7	32,2	56,2	60,0	28,0

6.4 Air velocity probing tests

The air velocity probing orienting map in fig 6.3 visualises the location of the measurements for the measurements in table 6.5, these showed an increase of 2 m/s at the inlet $V1$ from the base measurement in phase 2, when only the top part of the air rig were sealed. When only the bottom part of the air rig was sealed, a decrease in flow velocity at $V1$ from the base measuring was observed at 0,8 m/s. By sealing both the hopper and the bottom, the inlet velocity $V1$ raised by 2,75 m/s to 7,95 m/s, yielding the highest inlet velocity and throughput for phase 2. From these results, the hopper and bottom were enclosed and sealed better for phase 3 and together with other changes increased the inlet velocity V1 to 10.45 m/s. which is more than a 100% increase from the measured base inlet velocity at phase 2.

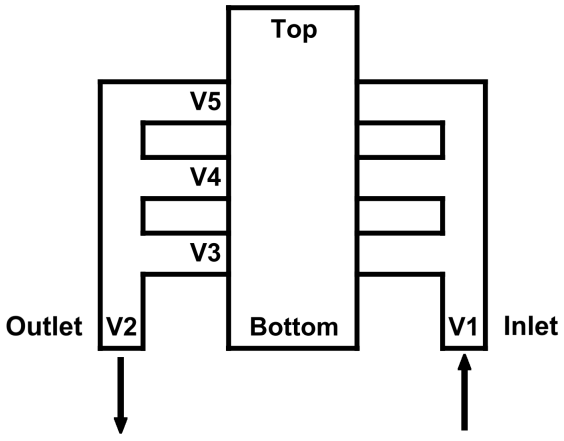

Figure 6.3: Air velocity probing test orienting map.

The base velocity measurements from phases 2 and 3 from table 6.5 both showed a

maximum outlet velocity of 16,6 m/s, which results in a volumetric flow of 235 m^3/h utilising equations 6.2 - 6.3, indicating that no condensation should occur according to the graph in figure 2.4 at 1% of moisture.

Table 6.5: Velocity probing test results.

Test	**Phase**	**V1 [m/s]**	**V2 [m/s]**
Base	2	5,2	16,6
Closed Top	2	7,2	16,3
Closed Bottom	2	5	16,3
Closed Top & Bottom	2	7,95	16,3
Base	3	10,45	16,6

A probing was conducted on the manifold of the air rig in phase 2 which showed a deviation among $V3$, $V4$ and $V5$ see figure 6.3. Table 6.6 shows the measured velocity values in the manifold, where the velocity is higher in the lower nozzles. The nozzles were sucking air from the rig where $V3$ was measured to 8 m/s, $V4$ to 4 m/s and $V5$ to 3 m/s. This leads to an uneven airflow through the rig which explains the temperature differences between the higher and lower sections of the air rig from table 6.4. The sum of $V3$, $V4$ and $V5$ adds up to 15 m/s which is a 1,6 m/s difference from $v2$ at 16,6 m/s. This difference could be explained either by friction losses or changes in the velocity profile due to deviations in the piping geometry in the shape of bends or valves. The change in velocity profile would alter the location of the maximal velocity and give deceiving measurements.

Table 6.6: Velocity manifold probing test results phase 2.

Phase	**V1 [m/s]**	**V2 [m/s]**	**V3 [m/s]**	**V4 [m/s]**	**V5 [m/s]**
2	5.2	16.6	8	4	3

6.5 Pressure estimation and validation

The following sections contain Calculations, measurements and results examining the hypothesis of a volumetric flow change due to pressure differences between the inlet and outlet of the air rig. The estimated height difference of the U-type manometer is compared through a validation with the measured height difference. The real pressure is also calculated.

6.5.1 Pressure estimation

The height difference of the U-type manometer water pillars were estimated for a volumetric change due to pressure, to explain velocity differences between inlet and outlet at phase 2.

Table 6.7: Parameters for U-type manometer pillar height estimation.

Variable	Value	Description
$\varnothing$	0.1 m	Inner pipe diameter
v_{1max}	5.2 m/s	Maximum pipe velocity at inlet
v_{2max}	16.6 m/s	Maximum pipe velocity at outlet
P_1	101325 Pa	Inlet pressure (Atmospheric)
ρ_1	1,2255 kg/m^3	Inlet air density (Atmospheric)
ρ_w	997 kg/m^3	Water density
Z_1	0 m	Initial pillar height
C_L	0.5	Averaging flow constant[14]

The cross sectional area A of the pipe is calculated from its inner diameter $\varnothing$.

$$A = \frac{\varnothing^2 \cdot \pi}{4} \tag{6.1}$$

The Maximum velocities v_{1max} and v_{2max} measured in the centre of the pipe cross section was averaged using the averaging constant C_L for laminar flows. Resulting in v_1 and v_2.

$$v_1 = v_{1max} \cdot C_L \,, \;\; v_2 = v_{2max} \cdot C_L \tag{6.2}$$

The volumetric airflows q_{v1} and q_{v2} are given as the product of the averaged velocities v_1 and v_2 together with the area A of the pipe cross section.

$$q_{v1} = v_1 \cdot A \,, \;\; q_{v2} = v_2 \cdot A \tag{6.3}$$

The mass flow m_1 at the inlet and m_2 at the outlet is given as the product of the respective volumetric flow q_{v1} ,q_{v2} and their densities. The density at the inlet ρ_1 was known due to the atmospheric air pressure.

$$\dot{m}_1 = q_{v1} \cdot \rho_1, \;\; \dot{m}_2 = q_{v2} \cdot \rho_2 \tag{6.4}$$

The mass flow at the inlet and outlet is assumed to be equal, which yields the density ρ_2 of the outlet as:

$$\frac{\dot{m}_1}{q_{v2}} = \rho_2 \tag{6.5}$$

From the perfect gas law and and constant temperature between inlet and outlet equation 6.6 is given.

$$\frac{\rho_2}{\rho_1} \cdot P_1 = P_2 \tag{6.6}$$

From the equation for hydro static pressure, equation 6.7 the predicted height difference ΔZ of the water pillar is calculated as:

$$\frac{P_1 - P_2}{\rho_w \cdot g} = \Delta Z \tag{6.7}$$

$$\Delta Z = 7,1073\, m$$

6.5.2 Pressure validation

The real pressure of the inlet is calculated using the observed height difference ΔZ of the water pillars.

Table 6.8: Parameters for pressure measuring.

Variable	Value	Description
P_1	101325 Pa	Inlet pressure (Atmospheric)
g	9,82 m/s^2	Gravitational acceleration
ρ_w	997 kg/m^3	Water density
ΔZ	0,02 m	Pillar height difference

Utilising equation 6.7. The real outlet pressure P_2 were calculated by inserting the measured water pillar height difference ΔZ, the inlet pressure P_1, the gravitational acceleration g and the density of water ρ_w.

$$P_2 = 101100\ Pa$$

The estimated pressure calculation indicated that in order to explain the velocity difference between the inlet and outlet at phase 2, a height difference in the U-type manometer pillars of 7,1073 m had to be observed between the outlet and inlet pressure. The pressure validation gave a height difference of 0,02 m which indicates that the velocity difference between the inlet and outlet is not due to volumetric change in the air but to losses from leaks and friction from an ineffective flow path. The real outlet pressure is calculated to 101129 Pa.

6.6 Mass balance

The flow of mass in phase 2 and 3 was calculated utilising the measured base values presented in 6.5.

6.6.1 Mass balance phase 2

A calculation of the mass flow difference between the inlet and outlet was carried out for phase 2 in order to observe the loss from leakages and friction. By assuming the inlet air pressure to be atmospheric, together with the measured pressure at the outlet and velocities for the inlet and outlet the mass flows could be calculated.

Table 6.9: Parameters for mass flow calculation phase 2.

Variable	Value	Description
$\varnothing$	0,1 m	Inner pipe diameter
$v_{1,max}$	5,2 m/s	Maximum pipe velocity at inlet
$v_{2,max}$	16,6 m/s	Maximum pipe velocity at outlet
P_1	101325 Pa	Inlet pressure (Atmospheric)
P_2	101129 Pa	Outlet pressure
ρ_1	1,2255 kg/m^3	Inlet air density (Atmospheric)
C_L	0,5	Averaging flow constant [14]

equation 6.1 - 6.3 were used to calculate the volumetric airflow q_{v1} and q_{v2}. from equation 6.6 could the air density ρ_2 at the outlet be calculated. With the respective densities and volumetric airflow could then the mass flow at inlet $\dot{m}_1$ and $\dot{m}_2$ at the outlet be calculated utilising equation 6.4

$$\dot{m}_1 = 0,02502\, kg/s\ ,\ \ \dot{m}_2 = 0,07973\, kg/s$$

6.6.2 Mass balance phase 3

From the pressure estimation and validation it was realised that the pressure differences inside of the rig are to small too have a significant impact on the density, for this reason a simplification was made in order to calculate the mass flows in phase 3 by assuming density at atmospheric pressure for both inlet and outlet while calculating the mass flow of air.

Table 6.10: Parameters for mass flow calculation phase 3.

Variable	Value	Description
$\varnothing$	0,1 m	Inner pipe diameter
$v_{1,max}$	10,45 m/s	Maximum pipe velocity at inlet
$v_{2,max}$	16,6 m/s	Maximum pipe velocity at outlet
ρ	1,2255 kg/m^3	Air density (Atmospheric)
C_L	0,5	Averaging flow constant [14]

equation 6.1 - 6.4 were used to calculate the mass flow $\dot{m}_1$ at the inlet and $\dot{m}_2$ at the outlet.

$$\dot{m}_1 = 0,05029\, kg/s\ ,\ \ \dot{m}_2 = 0,07988\, kg/s$$

6.6.3 Mass balance comparison

By calculating the mass flow of air at the inlet and outlet for phase 2 and 3 a comparison could be made. In phase 2, 31% of the airflow was retained at the inlet while 63% was retained at phase 3 which is a 100% increase of the mass flow of air through the system.

6.7 Energy balance

The energy balance for phase 2 and 3 were calculated using the measured velocity base values from table 6.5. The temperature values used to calculate the energy balance at phase 2 were taken from table 6.3 and the the values for phase 3 were taken from 6.4. A inlet temperature of 60 °C were used for both energy calculations as this was the highest documented temperature compatible between the phases.

6.7.1 Energy balance phase 2

Table 6.11: Parameters for calculation of energy balance phase 2.

Variable	Value	
$\varnothing$	0,1 m	Inner pipe diameter
$v_{1,max}$	5,2 m/s	Maximum pipe velocity at inlet
$v_{2,max}$	16,6 m/s	Maximum pipe velocity at outlet
C_L	0,5	Averaging flow constant [14]
T_1	60 °C	Inlet air temperature
T_2	38,5 °C	Outlet air temperature
T_{REF}	0 C	Reference temperature
ρ_1	1,059 kg/m^3	Inlet air density (60 °C) [16]
ρ_2	1,132 kg/m^3	Outlet air density (38.5 °C) [16]
C_p	1005 $\frac{J}{KgK}$	Specific heat of air[10]
$\dot{m}_1$	0,02502 kg/s	Inlet air mass flow
$\dot{m}_2$	0,07973 kg/s	Outlet air mass flow

The thermal energy flow Q1 and Q2 were calculated from the product of the relative temperature difference at the inlet respective outlet and the calculated mass flow from phase 2.

$$\dot{Q}_1 = \dot{m}_1 \cdot (T_1 - T_{REF}) \cdot C_p \,, \;\; \dot{Q}_2 = \dot{m}_2 \cdot (T_2 - T_{REF}) \cdot C_p \tag{6.8}$$

The kinetic energy flow were calculated with the mass flow at phase 2 and the averaged velocities given from equation 6.2.

$$KE_1 = \frac{1}{2} \cdot \dot{m}_1 \cdot v_1^2 \,, \;\; KE_2 = \frac{1}{2} \cdot \dot{m}_2 \cdot v_2^2 \tag{6.9}$$

The energy difference between the inlet and outlet were then calculated by subtracting the thermal and kinetic energy at the inlet from the energy at the outlet.

$$\Delta E = KE_2 + \dot{Q}_2 - KE_1 - \dot{Q}_1 \tag{6.10}$$

$$\Delta E = 1553,70W$$

6.7.2 Energy balance phase 3

Table 6.12: Parameters for calculation of energy balance phase 2.

Variable	Value	Description
$\varnothing$	0,1 m	Inner pipe diameter
$v_{1,max}$	10,45 m/s	Maximum pipe velocity at inlet
$v_{2,max}$	16,6 m/s	Maximum pipe velocity at outlet
C_L	0,5	Averaging flow constant [14]
T_1	60 C	Inlet air temperature
T_2	43,9 C	Outlet air temperature
T_{REF}	0 C	Reference temperature
ρ_1	1,059 kg/m^3	Inlet air density (60°C) [16]
ρ_2	1,113 kg/m^3	Outlet air density (43,9°C) [16]
C_p	1005 $\frac{J}{KgK}$	Specific heat of air[10]
$\dot{m}_1$	0,05029 kg/s	Inlet air mass flow
$\dot{m}_2$	0,07988 kg/s	Outlet air mass flow

The energy difference ΔE between the inlet and outlet were calculated utilising equation 6.8 - 6.10.

$$\Delta E = 582,44W$$

6.7.3 Energy balance comparison

From the temperature and velocity measurements in phase 2 and 3 the energy drop over the air rig could be calculated for both phases. In phase 2, 1554 W were lost while passing through the air rig while at phase 3 a loss of 582 W could be calculated. This is a 62,5% decrease in losses due to decreased thermal and kinetic energy loss.

6.8 Drying tests

The reference samples collected during the test series (see appendix C) shows that the moisture content of the unaltered -1mm crystalline dolomite is relatively stable, ranging from 0,10% to 0,14% (see tab. 6.13) of the total weight of the samples.

Table 6.13: Reference values from drying test phase 2 and 3.

Test	**Dry input** [g]	**Pre-drying** [g]	**Post-drying** [g]	**Ref. value** [g]	**moist.** [%]
3	3000,30	2997,95	2996,70	3,60	0,12
4	3000,00	2996,42	2995,63	4,37	0,14
5	3000,20	2998,26	2996,45	3,75	0,12
6	3000,10	2999,05	2997,02	3,08	0,10

As all tests were performed with an added moisture content of 1% (see tab. 6.14 - 6.16), the total moisture content of each test ranged from 1,1% to 1,14%. The tables

below contains all relevant drying test data gathered from the successful test series (appendix C), which was test series 3, 4, 5 & 6. It also details the temperature of the airflow at which the test was run, as well as the dry input weight, moist input weight, pre-drying weight, post-drying weight, and the calculated percentile moisture content after drying in the rig (moisture post-drying).

Table 6.14: Drying test results for phase 2 with one vacuum (outlet velocity 8.2 m/s).

Test	Temp [°C]	Dry input [g]	Moist input [g]	Pre-drying [g]	Post-drying [g]	Moist. post-drying [%]
3	23	3000,4	3030,7	2945,3	2924,6	0,71
3	30	3000,4	3030,7	2931,5	2911,8	0,68
3	30	3000,9	3031,2	2949,5	2928,8	0,70
3	40	3000,4	3030,7	2930,6	2911,1	0,67
3	40	3000,4	3030,7	2939,9	2921,4	0,63
3	50	3000,5	3030,8	2932,6	2914,4	0,63
3	50	3000	3030,3	2933,8	2916,6	0,59
3	60	3000,6	3030,9	2935,1	2916,1	0,65
3	60	3000	3030,3	2936,6	2918,4	0,62
5	70	3000,5	3030,8	2959,2	2939,2	0,68
5	70	3000,1	3030,4	2951,5	2931,9	0,67
5	80	3000,1	3030,4	2946,5	2926,2	0,69
5	90	3000,7	3031,0	2949,5	2929,9	0,67
5	100	3000,5	3030,8	2948,0	2928,8	0,66

Table 6.15: Drying test results for phase 2 with two vacuums (outlet velocity 16,6 m/s).

Test	Temp [°C]	Dry input [g]	Moist input [g]	Pre-drying [g]	Post-drying [g]	Moist. post-drying [%]
4	60	3000,1	3030,4	2913	2895,3	0,61
4	80	3000	3030,3	2908,7	2891,1	0.61
4	90	3000	3030,3	2905,3	2888,4	0,58
4	100	3000,1	3030,4	2893,3	2878,5	0,51
5	22	3000,6	3030,9	2917,7	2897,3	0,70
5	30	3000	3030,3	2909,2	2889,9	0,67
5	40	3000,6	3030,9	2909,9	2891,2	0,65
5	50	3000,1	3030,4	2912,1	2895,3	0,58
5	70	3000,3	3030,6	2897,4	2880,9	0,57

Table 6.16: Drying test results for phase 3 with two vacuums (outlet velocity 16.6 m/s).

Test	Temp [°C]	Dry input [g]	Moist input [g]	Pre-drying [g]	Post-drying [g]	Moist. post-drying [%]
6	25	3001,1	3031,4	2734,3	2720,7	0,50
6	40	3000,8	3031,1	2760,1	2746,1	0,51
6	60	3000,7	3031,0	2745,6	2735,2	0,38
6	80	3000,5	3030,8	2750,5	2743,2	0,27

Fig 6.4 illustrates the drying effect for the tests during phase 2 and 3 with the air rig. For the individual test points where we had several results, such as performing several tests at the same temperature with the same phase of upgrades, the average is displayed.

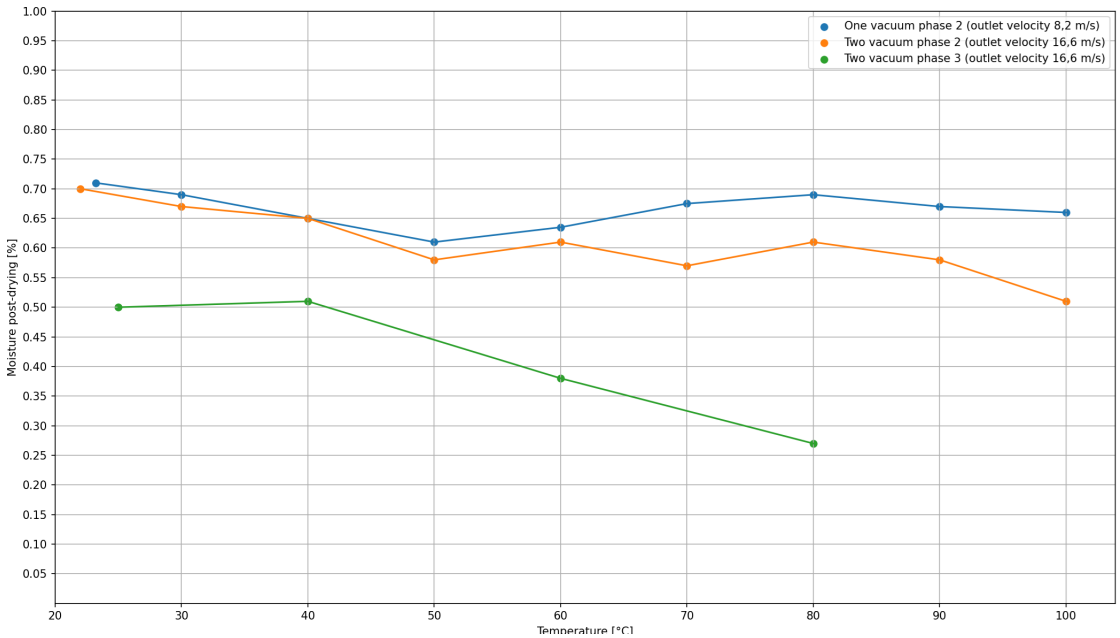

Figure 6.4: Graph illustrating moisture content after drying (in percentage) for drying tests in Phase 2 and Phase 3.

The blue plotted line from phase 2 with one vacuum, shows that the material's total moisture content evaporates down to 0,7% at room temperature. At the highest recorded temperature, 100°C, the material's total moisture content is only reduced to 0,65%. This indicates that the drying has reached a saturation level where the added heat is not effectively reaching the material, potentially due to cold air being drawn in from leaks.

The orange line from phase 2, using two vacuum cleaners, demonstrates evaporation down to 0,7% percent at room temperature. The material begins to stabilise around 0,575% at 50°C, deviating by approximately 0,025 percentage points until it drops to 0,5% at 100°C.

The green line from phase 3, using two vacuums shows that the material evaporates down to 0,5% at room temperature. There is no significant difference observed between room temperature and 40 degrees Celsius, but a clear downward trend is noted from 40 to 80°C, without any signs of saturated evaporation within this temperature range.

The minimal difference observed at lower temperatures between the lines in phase 2 suggests that the increased airflow did not have a direct impact on the evaporation process. This could be attributed to leakage and the air not effectively travelling through the curtain. However, the increase in airflow may have induced flow through the intake, as higher temperatures (70-100°C) resulted in more effective drying compared to lower airflow conditions.

In phase 3, a clear improvement in drying efficiency is observed due to better seal-

ing and a more efficient airflow path. This is evident from the room temperature measurements, which show a 0,2% lower total moisture content. Additionally, the increase in temperature has a more significant impact on drying because the increased airflow through the intake allows the heat to reach the material more effectively. This is further corroborated by temperature measurements at 60°C, where there is a 10-degree difference between phases 2 and 3 at the exhaust (using two vacuum cleaners).

Furthermore, at 80°C, the phase 3 air rig performed 63,5% better than the original setup of the air rig in terms of drying. This general trend of greatly improved drying can also be seen at room temperature, where no additional heat was supplied to the airflow but the drying performance of the phase 3 upgrades performed better than the drying effect of the original air rig setup at the highest heat tested, 100°C.

Due to the fact that the nozzles partially melted during the testing, more tests could not be performed past 80°C for the third phase of air rig upgrades.

6.9 Sieve analysis

The sieve test of the milled dolomite labelled as 1 mm gave the mass distribution among the particle sizes, which is tabulated in 6.17 and visualized in figure 6.5. From the mass distribution, the percentile mass distribution was calculated. Which showed that less than 2% of the sample were exceeding 1,4 mm. This resulted in a decision to set the roller gap to 1,5 mm to avoid material from jamming while passing in between the rollers. By adding up the percentile mass distribution for each mesh size, the cumulative particle size distribution was gained (see fig. 6.6). The cumulative particle size distribution shows the percentile distribution of particles which passes though the respective mesh size.

Table 6.17: Particle size distribution test results.

Mesh size [mm]	Mass distribution [g]	Distribution [%]	Cumulative [%]
2,8	0	0	100
2	0,07	0,07	99,93
1,4	1,63	1,55	98,38
1	8,37	7,97	90,41
0,71	22,94	21,84	68,57
0,5	14,59	13,89	54,68
0,355	8,99	8,56	46,12
0,25	9,54	9,08	37,04
0,18	8,93	8,50	28,53
0,125	8,89	8,46	20,07
0,09	6,28	5,98	14,09
0,063	5,54	5,27	8,82
0,045	3,07	2,92	5,89
$< 0{,}045$	5,24	5,89	NaN
loss($< 0{,}045$)	0,95		

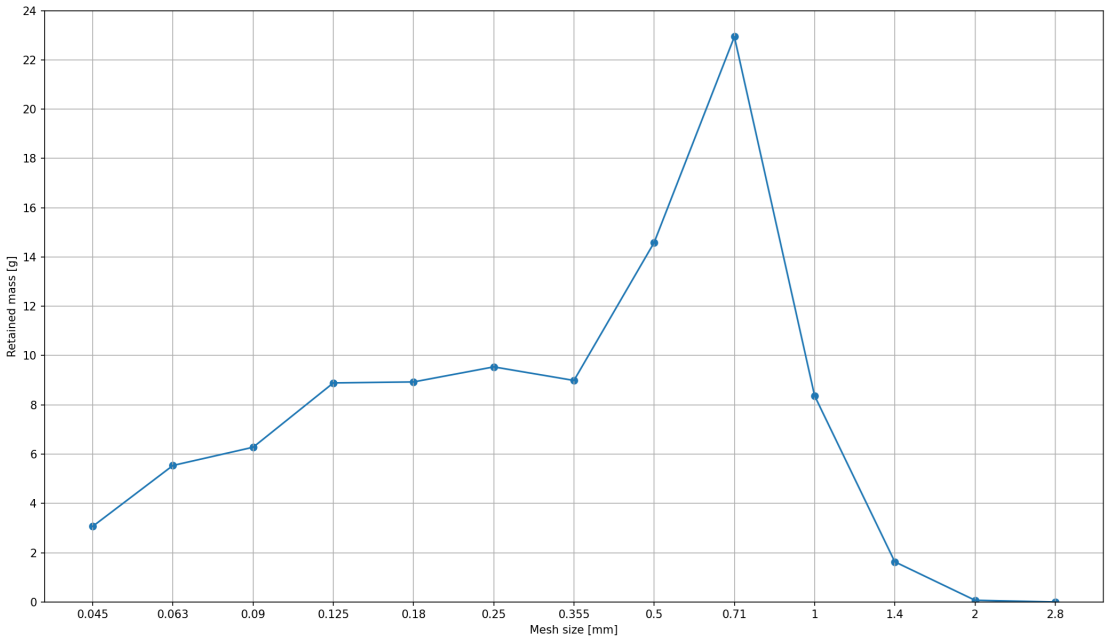

Figure 6.5: Particle size mass distribution, 1 mm dolomite.

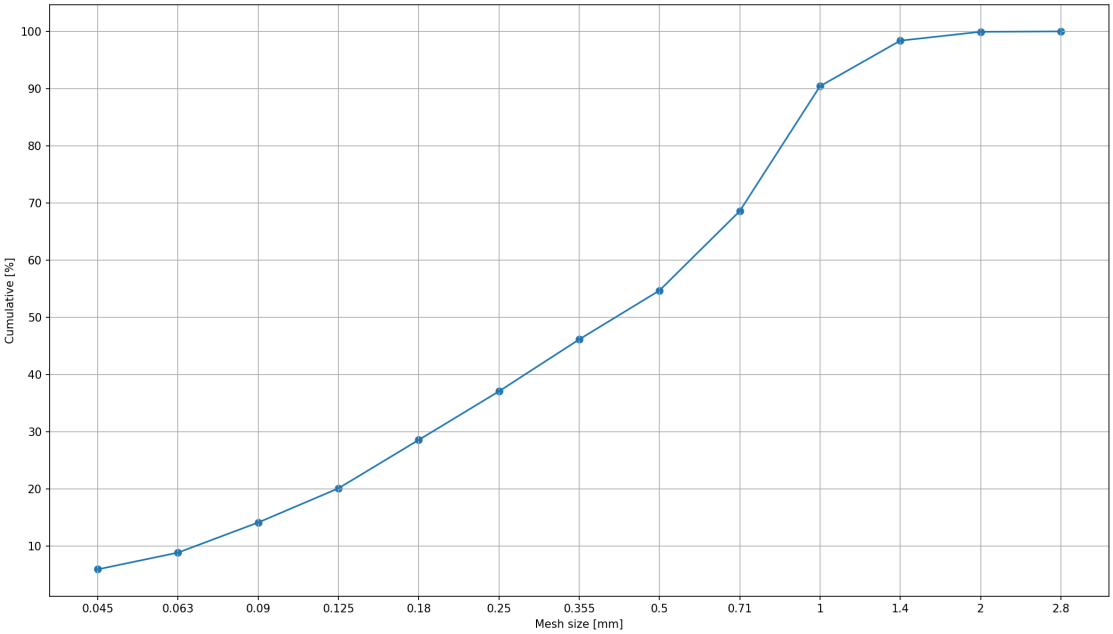

Figure 6.6: Cumulative particle size distribution, 1 mm dolomite.

The percentile material loss were calculated utilising equation 6.11. The major reason for the material loss is the removal of material fines from the cross-sectional flow. Small material particles are easier to move, as their low mass require less force and energy. For this reason, it is assumed that only the smallest material particles are removed during drying. The cumulative particle size distribution can then be used to evaluate the size of the particles that are removed for each drying test. In figure 6.7 the percentile material loss for each test can be seen. The red lines in the graph indicate the percentile of material removal that is required to remove particles of a certain size. These values were taken from the cumulative particle size distribution table 6.17.

$$Material\ loss = \frac{Dry\ input - Post\ drying - Reference\ value}{Dry\ input - Reference\ value} \tag{6.11}$$

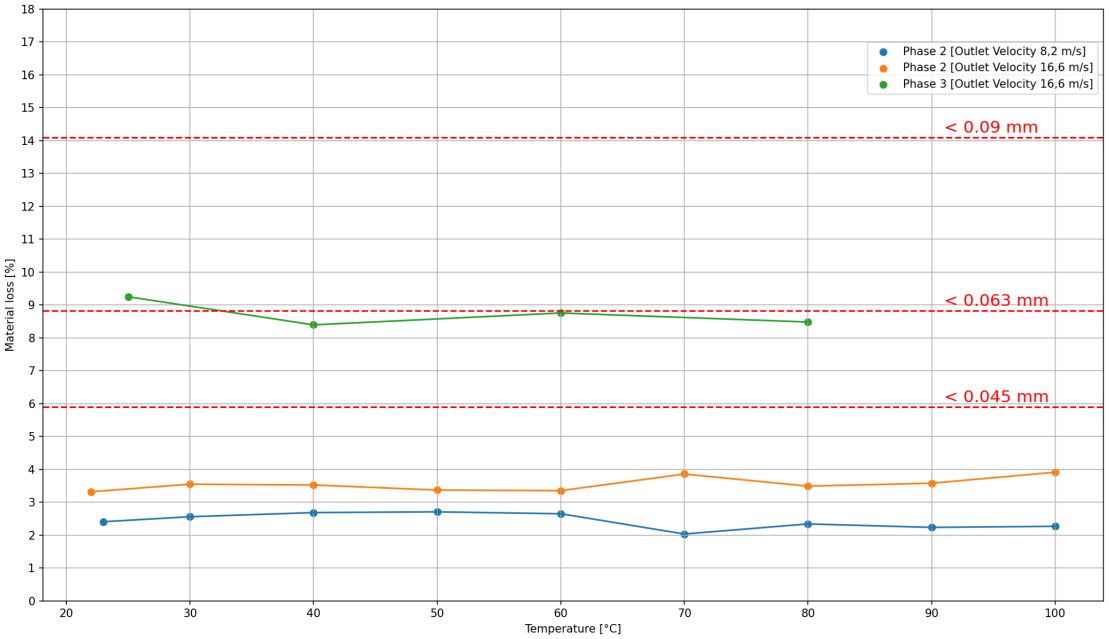

Figure 6.7: Percentile material loss at different temperatures in phase 2 and 3.

The tests from phase 2 show that no particles larger than 0,045 mm were removed by the cross sectional airflow. Tests in phase 3 showed a removal of about 9 % of material during drying, which indicates the largest particles to be of the size 0,063 mm or just below. There is no significant change in material loss with the different flow temperatures for any test series. The higher outlet velocity flow of 16,6 m/s from phase 2 gave an average material loss of 3,6%-while the lower one at 8,2 m/s yielded an average loss of 2,4%. From the increased flow from the upgrades in phase 3 an average material loss of 8,7% were calculated. This is below the 14% which indicates that no particles above 0,09 mm were removed and there by no particles above 0,1 mm, which is within the given restrictions.

6.10 Sustainability - Use2use

The full evaluation and results from the Use2use method can be viewed below in fig 6.8.

	Is it preferable for the user(s)?		Is it smart move for the organisation?		Is it good for the environment?	
	Potential **Will people be able to satisfy their needs better than today?** **How will people's activities and related practicalities change?** **Will people's costs be affected?**	**Implementation** **Will people have to change their everyday habits?** **Will people accept and adopt the change?**	**Potential** **How will it affect your revenues?** **How will your competitivness change?** **Will your brand be affected?**	**Implementation** **Will you have to change they way you do things** (processes, business logics, etc)**?** **Will you have to develop your strategic resources** (partners, competences, equipment etc)**?** **What are the risks involved?**	**Potential** **Will the use of virgin material or other resources change?** **Will the number of manufactured units change?** **What impacts will associated processes have** (distribution, remanufacturing etc)**?**	**Implementation** **Are there any environmental consequences connected to the implementation process?** **Are there any planetary boundries that can hinder implementation** (material scarcity etc)**?**
CONCEPT 17	People will indirectly be able to satisfy their needs better than today due to the potential cost savings getting passed down to the end customer. This could result in an increase in purchasing which could potentionally increase peoples satisfaction. The machine operators activities will not change drastically, as the proposed changes set in the final concept do not include advanced user controlls of any sort. Due to the nature of the ARBS mill, a customer will already save money in the long term due to how energy efficient the crushing mechanics are, together with the drying concept, the financial savings are great. With dry rocks, the crushing can keep operating at maximum efficiency and therefore retain the savings that were jeopardised with moist rocks.	Habits will not be changed with proposed design changes. The changes are relatively small in comparison to exisiting products and ex. material changes will not be noticed by the users so it will be accepted.	Although some of the costs might be slightly higher in production, the overall revenues should differ greatly. Due to the nature of the ARBS mill and its operation, the failure to provide adequate drying could end up costing more as it would require engineering-hours to solve. In this sense, if the final drying concept works practically, it could affect revenues positively. If the final drying concept ends up shipping with the ARBS mill, it could positively increase the mills competitivness. By rectifying the problems cause by moist material, a successful operational mill at an customer will positively impact an already strong (for an startup) brand.	The manufacturing processes need to change and adapt to the new materials and designs, but these changes are relatively minor. A slight development in strategic resources would be required in order to source all parts and equipment neccessary for the drying concept to work. Some of the risks involved are linked to the uncertainties regarding real world performance, specifically for the belt drying. These can be mitigated by performing additional test series in order to more accurately predict the drying performance. Apart from purely technical risks, there are no apparent large risks involved with moving forwards with the final concept.	Yes, because of the fact that the suggested concept involves additional parts, more material will be used for the construction of the final mill. But as these mills are not currently mass produced, the environmental impact is deemed to be minor. The number of manufactured units will not change unlesss there is an sudden increase in sales. The associated processes will have low overall impacts on the environment because the mill is not mass produced. The transport of manufactured goods to the work site will be slighly greater, but still small in relation to other processes in the mining industry, such as mining and transporting of rocks.	There is a large beneficial environmental consequence connected to the implementation due to the fact that residual heat/waste heat is utilised for the drying, heat that could otherwise go to waste. Reusing and recycling from a manufacturing process can be incredibly energy efficient, and in this case, utilising waste heat removes the need to generate heat using electricity, which yields great savings in potential energy cost. A consequence of utilising this waste heat for drying is that this very heat could have been used for heating up buildings, but as it is allocated towards the drying of material, the buildings will have to use another source of energy for heating. No planetary boundries exist that could hinder implementation of the final concept.

Figure 6.8: A visualisation of the Use2use evaluation.

7
Discussion

7.1 Methodologies

Due to the fact that many of the tests performed were developed for this thesis, the iterative nature of developing these methods meant that some of the earlier tests were not as efficient and/or meaningful. With the methods developed for evaluating drying, further testing will prove less time consuming while also yielding results that are far simpler to evaluate. This is made easier by the developed test data evaluation methods, including the spreadsheet templates developed during the project.

Optimisation and tuning in our testing methods were made continuously during testing and resulted in efficient, safe testing. This also means that the tests that were not performed due to time limitations, such as tests in Boliden on the pilot plant and general drying tests on a conveyor will probably suffer from not being properly developed yet.

7.2 Results

Mass balance
The mass balance evaluation that could be performed for the different phases, due to the airflow measurements, showed a twice-as-large amount of air that is pulled through the inlet where heat is supplied. This took place after the top and bottom of the air rig were sealed, and the wall-crushing element slit distance was minimised. This caused the general air tightness of the rig to increase.

When the mass flow is directly dependent on the flow velocity, it is possible to deduce that approximately half of the increase in mass flow of air is due to the encasement of the top and bottom of the air rig. The other half of the increase in air mass flow came from the improved general sealing of the air rig in phase 3 and the reduced wall/crushing element slit distance. Which indicates that a properly sealed module with an efficient flow path is crucial for the implementation of a drying system.

Energy balance
The energy balance, which included thermal and kinetic energy, was calculated using airflow and temperature measurements, showing the loss between the inlet and outlet had decreased to 37% after the upgrades from phase 2 to phase 3. Given that

this work aims at "waste heat utilisation," it is crucial to use the supplied energy efficiently, minimising losses as much as possible. Since the outflow from the rig still retains heat, there are opportunities to further utilise the waste heat from the drying process, thereby enhancing the system's efficiency.

Insulation test
The insulation test that was performed showed clear indications that thermal energy could be saved by insulating the duct piping, even over a short distance of 1650 mm. The test was conducted with a significantly lower flow velocity than that required for drying in the mill. Utilising a higher flow velocity would result in a lower temperature drop, as the air has less time to cool when travelling the same distance. Therefore, it is important not to directly correlate the temperature drop during the insulation test to that in the mill, but rather to consider it as an indication that insulation significantly reduces thermal losses, which would increase with longer pipe lengths. This is important to consider when the drying system is introduced to the mill. A minimised total piping length, combined with insulation, will further reduce energy losses.

Rig heat temperature and heat permeability
From the temperature measurements in the rig, it is evident that the overall temperature at the same intake temperature has increased with the upgrades. The highest temperature recorded inside of the air rig was measured to 60°C, which leaves a headroom of 20 degrees before exceeding the restrictions set by the requirement specification. An overview of the temperature distribution in the rig shows that the temperature is higher further down in the rig. From the flow rate measurements in the manifold, it is observed that the flow rates are higher at the lower inlets. This indicates that the uneven flow distribution in the manifold directly affects the flow temperature. The uneven temperature and flow distribution cause the drying process to be inconsistent. By equalising the distribution of the airflow by redesigning the manifolds, a more uniform process could be achieved, which would facilitate easier evaluation of optimal air velocities and temperatures.

Drying tests The drying tests clearly showed that a large amount of drying can be performed inside of the mill. This is important as it indicates that the implementation of drying in the ARBS mill is possible. This finding came in part due to the upgrades brought forward in phase 3 that yielded a significantly increased drying effect resulting in an 75% decrease of moisture left the crushed rock material. This drying was performed with temperatures below the maximum allowed temperature inside of the machine, which exists in order to not overheat the sensors in the mill.

It is still unclear where the airflow temperature limit, i.e. the upper boundary of the temperature of the supplied air that will not lead to temperatures inside of the machine above the maximum allowed temperature, which is 80°C. This lack of data at is due to the failure of the plastic inlet nozzles, but it is evident that there is headroom to increase heat further to achieve a possibly higher degree of drying.

Had time and the failure of the nozzles not been an issue, further research and testing using larger rock sizes would have been performed, which could have yielded results that could give a better understanding of how drying works on different material sizes and at higher temperatures. While higher temperatures was possible using the phase 1 and phase 2 air rigs, the phase 3 air rigs heat retention was so efficient that the inner temperature far exceeded that of phase 1 and phase 2.

Looking at graph 6.4, it is evident that upgrades brought forward in phase 3 improved drying and it shows the importance of properly sealing the machine and insulating heat transfer pipes on any future mills. The sealing and insulation will reduce the required heat and airflow necessary to dry the material to reach a satisfactory moisture content.

For the drying tests in phase 2, a discernible saturation of the evaporated moisture was observed, as can be seen in the drying graph 6.4, where increased temperatures barely yielded a higher degree of drying. For phase 3 testing on the other hand, higher temperatures yielded significantly higher drying rates without any signs of saturation, suggesting that higher temperatures could have yielded even higher drying rates.

Graph 2.4 show the required volumetric airflows and temperatures required to evaporate the necessary amount of water. With the volumetric airflows and temperatures used in the drying tests, it is evident that there is a large headroom for the transported evaporated moisture.

7.3 Final concept

The final concept incorporates the original idea of drying the material curtain with a heated airflow, a concept that can be easily incorporated into any current designs at CR while using the waste heat provided from latter stages on a mineral processing plant. It also adds conveyor drying in order to avoid sending in material that is too moist, as a sub 1% moisture content is required for the mill to maintain full efficiency. The conveyor drying is simple in both implementation and design, as it relies on a number of sheet metal covers with insulation that are mounted on top of the conveyor belt, allowing hot air to flow through the material as it is being transported to the crushing stage.

7.4 Sustainability

The premise of the project as well as its name suggest using waste heat to increase the crushing/milling efficiency of the ARBS mill, a machine that already touts significant reductions in consumed energy. This premise set the tone for the project from the start by being a key part of the green revolution in the mining industry.

8

Conclusion

This chapter covers the conclusions of the thesis project as well as general recommendations for further development.

8.1 Conclusions

The project (as laid out in 1.2) consisted of four aims.

The first aim was to measure the degree of drying that can be achieved under a range of operating conditions. This aim was mostly fulfilled due to the magnitude of tests that were performed on different aspects of the air rig and its surrounding systems. Although the range of drying is better understood now, there is still a lot to learn about the drying in not only the air rig, but the ARBS mill as well. This knowledge is ideally gathered by conducting further testing with a larger variety of input variables to clearly retrieve saturation points of evaporation in the ARBS mill.

The second aim was to understand and quantify the operating parameters and machine design elements that enhance or diminish the drying effectiveness, and these have largely been identified and/or quantified, to a lesser degree. There is a general lack of knowledge when it comes to understanding how a mathematical model of drying for the ARBS mill would work, with time and a lack of knowledge regarding the airflows inside of the air rig being the restricting factors. With a better understanding of the drying and operating parameters, a complete mathematical model could be developed for Comminution Reimagined's ARBS mill.

At a specific airflow rate in the rig, evaporation saturates at a sufficiently high temperature. This temperature must be determined through testing. Therefore, more tests are necessary to find an airflow rate and temperature that provide high drying efficiency without consuming large amounts of energy. Since evaporation is affected by all conditions in the machine, these tests should be conducted on the actual crusher to obtain relevant values with different particle sizes, etc.

It is also important to recognise that good airflow through the curtain is essential, as well as having an airtight and well-insulated system. This goes not only for any future testing but more importantly for any future mills. Test data also suggest that temperature has little impact without sufficient airflow, but with adequate airflow, it becomes more significant. Tests also show that there is potential to increase the

airflow significantly without risking excessive extraction of material fines.

The third aim was to propose a set of changes to the mill design to enable the incorporation of effective air drying into the first delivered mill, which is mostly fulfilled as this project proposes a concept. This concept still requires testing and optimising, but complexity of the concept is relatively low, which allows CR to test it out without allocating to much in terms of engineering hours or cost.

The fourth and final aim was to ideally, incorporate the proposed changes into the final mill design. This aim was not achieved due to time constraints. Since the final concept still requires testing and fine tuning, it is not reasonable to suggest design changes to the final mill design. While the final concept requires some minor design changes to the final mill, proposing them and implementing them at this stage could cause issues down the line due to the concept not being fully tested.

Due to the relative short nature of this project, several additional steps have been planned out in order to verify results and ensure that the final concept can be applied to a end-customer mill. The continuation of the testing regime initiated during the project would act as a starting point for Comminution Reimagined to finalise the project that was started with this thesis.

Overall, there is satisfaction with the results and the fulfilment of the set aims. Time being a limiting constraint affected the possibility of performing more tests, getting a better understanding of the drying effect and implementing a set of proposed changes of the final mill design. It is clearly evident that drying of the nature that is suggested is mature enough to a point where it would be beneficial for CR to continue their pursuit into drying based on our findings. Drying is a necessary component of CR mill today and the work laid out during this project will ensure that CR does not have to start from the beginning.

Bibliography

[1] Gustaver, M. (2020). A Chalmers University of Technology Master's thesis template for LaTeX. Unpublished.

[2] Vem, när, vad, var

[3] Comminution Reimagined. (2024). *About Our Company.* Retrieved April 22nd, 2024, from https://www.comminutionreimagined.com/about

[4] Comminution Reimagined. (2024). *Technology - ARBS.* Retrieved April 23rd, 2024, from https://www.comminutionreimagined.com/about

[5] Tsotas, E., Gnielinski, V., Schlunder E. U. (2005). *Drying of Solid Materials* Retrieved May 25th, 2024, from https://ethz.ch/content/dam/ethz/special-interest/mavt/process-engineering/particle-technology-laboratory-dam/documents/lectures/practica/lecture-documents-2016/Additional_theory.pdf

[6] Parikh, D. M. (2014). *Solids drying: Basics and Applications.* Retrieved May 25th, 2024, from https://www.chemengonline.com/solids-drying-basics-and-applications/?printmode=1

[7] Putra, R. N., Ajiwiguna, T. D. (2017). *Influence of Air Temperature and Velocity for Drying Process. Journal of Procedia Engineering 170 (2017) 516 – 519.* https://doi.org/10.1016/j.proeng.2017.03.082

[8] Libal, A. (2018). *What Happens to Air Pressure With an Increase in Water Vapor?* Retrieved May 27th, 2024, from https://sciencing.com/happens-air-pressure-increase-water-vapor-22855.html

[9] Schmitz, M., Biermann, M., Normann, F. (2020) *Formel- och tabellsamling Termodynamik med Energiteknik.* Department of Energy Technology, Chalmers University of Technology.

[10] Schmitz, M., Biermann, M., Normann, F. (2020) *Formel- och tabellsamling Termodynamik med Energiteknik.* (pp. 3). Department of Energy Technology, Chalmers University of Technology.

[11] Singh, P. (2024). *Absolute Humidity Calculator.* https://www.omnicalculator.com/physics/absolute-humidity

[12] The Engineering ToolBox (2004) *Universal and Individual Gas Constants.* [online]. Retrieved May 25th, 2024, from https://www.engineeringtoolbox.com/individual-universal-gas-constant-d_588.html

[13] Geo for CXC. (n.d.). *Limestone Features.* Retrieved June 20th, 2024, from https://geoforcxc.com/water/limestone-features/#google_vignette

[14] Engineering Library. (n.d.). *Laminar and Turbulent Flow*. Retrieved June 5th, 2024, from https://engineeringlibrary.org/reference/laminar-and-turbulent-fluid-flow-doe-handbook

[15] Meriam Instruments *via* Transcat. (n.d.). *Manometer Principles*. Retrieved June 21st, 2024, from https://www.transcat.com/calibration-resources/application-notes/manometer-meriam-principles

[16] Engineers Edge. (n.d.). *Properties of Air at 1 atm Pressure*. Retrieved June 3rd, 2024, from https://www.engineersedge.com/physics/properties_of_air_at_1_atm_pressure_13828.htm#google_vignette

[17] Ballast, SIS/TK 187. (2012). SS-EN 933-1:2012. *Tests for geometrical properties of aggregates - Part 1: Determination of particle size distribution - Sieving method*.

A

Requirement specification

The full requirement specification can be found in on the following page.

CHALMERS *Requirement specification*

Nr	Name	Interested Party	D/W	Rating of wish (1-5)	Function	Description
					Moisture content	
1	Material moisture content - output	CR	D		Output moisture content	Allowed moisture content post crushing
2	Material moisture content - output	SMA	D		Output moisture content	Allowed moisture content post crushing
3	Material moisture content - input demand	CR	D		Pre crushing moisture content	Allowed moisture content pre crushing
4	Material moisture content - input wish	CR	W	4	Pre crushing moisture content	Optimal moisture content pre crushing
					Temperatures	
5	ARBS mill core temperature	CR	D		ARBS temperature	Allowed general temperature of the ARBS mill
6	Conveyor belt heat	CR, SMA	W	3	4-stage conveyor temperature	Temperature of the 4-stage conveyor belt
7	Input air flow temperature	SMA	D		Input air temperature	The temperature of the delivered air from SMA Mineral
					Cost	
8	Proposed concept cost - demand	CR, SMA	D		Drying solution cost	The total cost of the drying solution implementation, demand
9	Proposed concept cost - wish	CR, SMA	W	3	Drying solution cost	The total cost of the drying solution implementation, wish
					Time	
10	Effective drying time	CR, SMA	D		The time material has to dry is during its journey through the sy	Time available for drying
					Particles	
11	Allowed particle size for removal via air	CR	D		Fines particles removal size	Only particles of a certain size is allowed be removed from the mill during crushing
					Environmental	
12	Energy consumption - Waste heat	SMA	W	2	Waste heat consumption	Energy suplied from waste heat
13	Enegy consumption - Additional energy	CR, SMA	W	4	Additional heat consumption	Additional energy needed to drive drying process
14	Energy efficiency	SMA	W	3	Energy efficiency	Efective utelization of energy suplied
15	Underpressure in machine	CR	D		Maintaining underpressure	The machine must sustain underpressure to not blow out dust
					Construction	
16	Ease of assembly	CR, SMA	W	3	Easy assembly	Ease of assembly of the drying solution
17	Compatible with current system	CR, SMA	D		System compatability	Drying solution compatability with the ARBS mill
18	Resistant to dust	CR, SMA	D		Dust resistance	Dust resistance of the drying solution
19	Resistant to outdoor enviroments	CR, SMA	D		Outdoor weather resistance	The drying solutions resistance to the elements
					Maintenance	
20	Maintnance intervals that concur with other maintnance	SMA	W	2	Maintanance interval	The maintenance interval needs to align with the ARBS mills.
21	Parts that are introduced to wear easy to replace	CR, SMA	W	2	Easy replacement	Ease of replacement of parts that could wear
					Safety	
22	Low risk of injury	SMA	D		Operator injury risk	Risk for operator injury
					Operation	
23	Easy to operate	SMA	W	3	Operation ease	Ease of usage for the drying solution
24	Adjustable drying	SMA	W	3	Drying adjustability	Adjustability of the drying effect and its parameters
25	Predictive drying	CR, SMA	W	4	Drying predictability	Predictability of the drying effect

Latest revision date: 2024-05-18

Verification method	Target value	Unit	Comment
Drying tests	0,0-0,3	[%]	Desired final moisture content. As moisture content gets reduced, general crushing efficiancy is increased. Therefore it's desirable to dry the material as soon as possible, as much as possible
Drying tests	< 1	[%]	Accepted final moisture content for SMA. A higher moisture content than 1% could cause issues with the transportation of material to the furnace.
Drying tests	< 2	[%]	Accepted moisture content before any crushing. A higher moisture content will cause issues with crushing efficiancy early on in the crushing stage.
Drying tests	0	[%]	
Measurements from heat tests	< 80	[°C]	Due to the heat sensititivy of the various sensors inside of the ARBS, the temperature of the ARBS may not exceed 80°C.
Measurements from heat tests	Minimise heat	[°C]	Reaching max drying effect without wasting heat is imperative as higher temperatures around the conveyor belt results in more frequent service.
Temperature test	<=120	[°C]	
Cost assessement	< 10,000,000	[SEK]	The proposed drying solution needs to be significantly cheaper than a market solution, due of the nature of the project being a general cost saving.
Cost assessement	Minimise cost	[SEK]	
Design evaluation	Inside mill	N/A	The drying needs to take place between CRS the mill recieving the feed material and when the crushed rocks are sent of to the oven.
Sieving of cyclone fines	< 100	[µm]	
Energy flow estimation by massflow and temperature	Minimise	[W]	
Data sheet evaluation	Minimise	[W]	
Energy balance calculation	Maximise	[%]	
	Yes	[Yes/No]	
DFA	Yes	[Yes/No]	
CAD model	Yes	[Yes/No]	
Pressure test	Yes	[Yes/No]	
Material selection	Yes	[Yes/No]	
Maintanance analysis	As current machine	N/A	
FMEA	Yes	[Yes/No]	
FMEA	Minimse risk	N/A	
Operator feedback	Yes	[Yes/No]	
Design evaluation	Yes	[Yes/No]	
Design evaluation	Yes	[Yes/No]	

B

Pugh matrix

CHALMERS	*Pugh Matrix 1*								
Latest revision date: 2024-03-18									
Requirements	**Concepts**								
	11	8	9	10	14	15	16	17	18
Feasability		-	-	-	0	-	-	+	-
Compatability with current system		-	-	-	+	-	0	0	0
Simplicity	R	-	-	-	-	-	-	-	-
Energy efficiency	E	+	+	+	+	-	+	+	+
Integrability	F	0	-	-	+	-	0	0	0
Technological maturity	E	0	0	0	0	0	0	0	0
Low cost of implementation	R	-	-	-	+	-	0	0	0
Environmental impact of implementation	E	0	0	0	+	-	0	+	0
Maintanance and effect on current maintanance schedule	N	0	0	0	0	-	0	0	0
Have enough information	C	-	+	0	0	0	0	0	0
Σ +	E	1	2	1	5	0	1	3	1
Σ 0		4	3	4	4	2	7	6	7
Σ -		5	5	5	1	8	2	1	2
Net value		−4	−3	−4	4	−8	−1	2	−1
Rank		**6**	**5**	**6**	**1**	**8**	**3**	**2**	**3**
Comment		Vapour removal?							
Decision		Rem.	Rem.	Rem.		Rem.			Rem.
Reflection	Combining different solutions to cover more of the design space?								

C

Drying test notes

This appendix contains the notes from the 6 drying test series.

A total of 57 tests samples of 3000 grams of dolomite were prepared and 27 tests were completed successfully during 6 test series. The text below describes the 6 test series that were performed.

Test series 1
The first test series took place early on during the pre-study phase of the project, in Q4 2023. The test series was led by engineers at CR and had two purposes, to introduce the thesis workers to the work at CR and to get an early indication of the potential performance of drying crushed rock material using hot air. This was the only test series that was led by employees of CR. The results from this pre-study test series were not taken into account during the data evaluation due to the tests lacking the test structure that was later developed for test series 2 and forward. The first test series consisted of 3 prepared tests, one of which was the reference, used to determine the initial moisture content of the crushed rocks. Test series 1 used -1mm crystalline dolomite.

Test series 2
The second test series consisted of 4 prepared tests, of which one was a reference sample. Due to bridging, a term used for when material fails to enter the crushing chamber due to the blockage of the entrance of said chamber, the first prepared test failed and the blockage caused one of the crushing element motors to fail. This necessitated a motor swap, which led to the cancellation of the rest of the test series. The cause of the bridging was determined to be due to the slit distance of the hopper being to large, leading to a higher than usual material flow. In order to curb the material flow and prevent another bridging failure, a material flow test 3.2 was conducted in connection with test series 2 to ensure that future tests could succeed. The air rig went through the first phase (5.2) of upgrades at the same time as the motor got replaced. Test series 2 used -1mm crystalline dolomite.

Test series 3
The third test series consisted of 10 prepared tests, of which one was a reference sample. This test series utilised one (1) vacuum unit on all prepared tests. This test series evaluated the drying effect on lower temperatures, with airflow temperatures between room temperature and 60°C. Test series 3 used -1mm crystalline dolomite. All tests were performed successfully and the results of the tests were used in the

data evaluation.

Test series 4
The fourth test series consisted of 7 prepared tests, of which one was a reference sample and another prepared test was used for a material flow test to ensure that the test rig kept the desired material flow set using the results from Test series 2. This test series utilised one (1) vacuum unit on all test prepared tests. The main purpose of this test series was to investigate the drying effect on higher temperatures, with airflow temperatures ranging from 60°C to 110°C. The modified construction heater could not push temperatures above 100°C due to a lack of effect. This led to the cancellation of the final prepared test, which yielded no result for 110°C. Test series 4 used -1mm crystalline dolomite.

Test series 5
The fifth test series consisted of 11 prepared tests, of which one was a reference sample. This series utilised both one (1) and two (2) vacuum units in order to be able to evaluate the effect of airflow on the drying rate. This test performed drying tests with airflow temperatures ranging from room temperature (circa 23,2°C) to 100°C. The entire test series was performed successfully. The fifth test series was the first to utilise the upgrades brought forth in the second phase of the prototyping (5.3) and it used -1 mm crystalline dolomite.

Test series 6
The sixth and final final test series consisted of 22 prepared tests, of which two were reference samples. The use of two reference samples are due to the inclusion of a new crushed rock size, the same crystalline dolomite in 3-5 mm. This series utilised two (2) vacuums units. The main purpose of this test series was to investigate the drying temperature on high temperatures for -1mm dolomite. A secondary purpose was to evaluate the difference in drying effect and rate for material size ranges. The test was supposed to start by running -1mm dolomite through the air rig at temperatures between room temperature and 130°C. The higher temperatures were thought to be possible due to the effects of the third phase of upgrades mandated a sixth test series. Due to improved heat retention inside of the air rig that came with phase 3 (5.4), the plastic nozzles started to deform when the construction heater was set at 90°C. This occurred after the 4th prepared test and necessitated an early test series abortion. Out of the 22 tests, 5 prepared tests were performed successfully, including one reference sample.

DEPARTMENT OF SOME SUBJECT OR TECHNOLOGY
CHALMERS UNIVERSITY OF TECHNOLOGY
Gothenburg, Sweden
www.chalmers.se

CHALMERS
UNIVERSITY OF TECHNOLOGY